by the host NMD machinery. Moreover, we found that HTLV-1 has evolved mechanisms to override and escape the host NMD pathway. We provide evidence that HTLV-1 Rex plays a critical role in the suppression of host NMD activity.

Firstly, we demonstrated that the host-encoded NMD specifically targets HTLV-1 genomic RNA and primary transcripts for RNA turnover. Therefore, host NMD acts to reduce viral structural gene expression and perturbs virus production. The steady-state expression of HTLV-1 unspliced mRNA showed a negative correlation with cellular NMD activity (Fig. 1A), and the stability of unspliced viral mRNA was highly sensitive to cellular NMD activity (Fig. 1B). Luciferase reporter assays, in which the luciferase activity reflects the stability of a *gag*-derived fragment of HTLV-1 genomic RNA, showed that the stability of HTLV-1 *gag* mRNA was directly influenced by the cellular level of UPF1 or UPF2, the key positive regulator of NMD (Fig. 2). Many researchers have demonstrated that UPF1 phosphorylation by the serine/threonine kinase SMG1 facilitates triggering of NMD and exclusion of aberrant mRNAs from the normal translational pathway. These mRNAs are redirected to the P-body, where they await targeted turnover [21,22]. UPF1 plays an important role in discrimination of PTCs that are positioned upstream of EJC at the last exon–exon boundary of spliced mRNAs and selectively activates the NMD machinery for degradation of the targeted mRNA [23]. Recognition of PTC by UPF1 is achieved by interaction of UPF1 at the termination codon with UPF2/UPF3 at EJC, which becomes possible only when a termination codon is positioned upstream of EJC. In yeast, the P-body is the major site for PTC-containing aberrant mRNAs awaiting degradation [24–26]. In mammalian and human cells, all NMD components localize to P-bodies [21] and phosphorylated UPF1 accumulates at these structures [22], supporting the notion that P-bodies accumulate mRNAs targeted for NMD turnover in mammalian cells. Taken together, accumulating evidence indicates that UPF1 is the key regulator in discrimination, selection, and translocation of aberrant mRNAs to P-bodies where they await degradation [21–23,26,27]. The results in the present study demonstrate that phosphorylated UPF1 interacts with HTLV-1 unspliced RNA with a high affinity and the HTLV-1 unspliced RNA complex accumulates in P-bodies (Fig. 1C and D). Our results thus indicate that HTLV-1 genomic RNA is detected by UPF1 as are other cellular NMD target mRNAs and transferred to P-bodies for degradation. Consistent with this notion, NMD antagonized efficient HTLV-1 replication (Fig. 1A and B), whereas the suppression of NMD activity led to a significant increase in HTLV-1 Gag proteins, p53, p24, and p19 (Fig. 6C). Thus, NMD destabilizes HTLV-1 genomic RNA and reduces the expression of viral structural proteins, presumably leading to a reduction in viral particle formation.

Several reports raise the possibility that retroviral transcripts are selectively targeted by the host mRNA decay mechanism, and they have unique or overlapped strategies to avoid degradation. Viral mRNAs of Rous sarcoma virus (RSV) [28] and human foamy virus [29] are selectively degraded in the host cell, although the authors of those studies concluded that the degradation may be accomplished by pathways distinct from NMD. Ajamian et al. reported influence of host encoded NMD-factor, UPF1, on unspliced HIV-1 mRNA, intriguingly enhancing the stability of HIV-1 mRNA [30]. Hogg and Goff proposed a possible model that 3′ UTR-length-dependent accumulation of UPF1 functions as a mark of potential mRNA-decay target [31]. The authors speculated that retroviruses may take advantage of this host-encoded system by employing in-frame read though and/or frame-shifting, which prevents steady-state UPF1 interaction and RNP composition, thus disrupts recognition of the viral mRNA as a decay target. In addition to these previous reports, our data show that unspliced HTLV-1 RNA is a target of a powerful host-encoded mRNA decay mechanism, NMD, and for efficient replication and propagation of new viral particles, it is critical for HTLV-1 to evade the NMD pathway.

On confirming that the host NMD pathway represents a significant impediment to efficient HTLV-1 replication, we posed the critical question: has HTLV-1 evolved a strategy to evade NMD? We observed that HTLV-1-infected cell lines have significantly lower basal NMD activities than HTLV-1-unrelated cell lines (Fig. 3B), implying that HTLV-1 infection may influence host NMD activity. Indeed, the NMD activity was notably suppressed by HTLV-1 infection or protected by inhibition of HTLV-1 infection via AZT treatment (Fig. 3C–E), suggesting the existence of viral factor(s) that suppress the host NMD pathway. Besides the structural proteins, HTLV-1 encodes regulatory and accessory proteins (Tax, Rex, p30II, p12, and p13) in the pX region of the genome. The functions of those proteins have been well studied and reviewed [32,33]. Tax is a multifunctional oncoprotein and transcriptional transactivator that regulates both viral and cellular gene expression [34,35]. HTLV-1 Rex is a virus-encoded, high-affinity, RNA-binding protein that binds

On the other hand, the luciferase activity of PTC-Glo, of which transcript is NMD target, can be detected only under NMD inhibition. The reporter is sensitive to changes in NMD activity in HeLa cells (right panel). Data from three independent experiments are shown ($n = 3$, mean ± SD; $^{***}p < 0.001$). (B) NMD activities were measured by β-globin-based NMD reporter assays in control fibroblasts (HeLa and TIG-1), control T-cell lines (Jurkat and CEM), HTLV-1-transformed cell lines (MT-2 and ATL2), and ATL-derived cell lines (TL-Om1 and KOB). HTLV-1-infected T cell lines show significantly lower NMD activities compared with HTLV-1-unrelated cell lines. Data from three independent experiments are shown ($n = 3$, mean ± SD; $^{**}p < 0.01$). (C) The course of HTLV-1 expression in sHeLa cells co-cultured with MT-2. *Gag* or *tax/rex* mRNA by RT-PCR (left panel) as well as Tax and Rex protein levels determined by Western blotting (right panel) show peaked viral expression 1 and 2 days after infection. (D) NMD activity was measured via dual luciferase assays in HTLV-1 infected sHeLa cells and compared with that in uninfected control cells. Gray circles indicate the results from uninfected control cells, while black circles represent data from HTLV-1 infected cells. Significant NMD inhibition was observed on the first ($p < 0.05$) and second ($p < 0.01$) days after HTLV-1 infection. Results shown are from three independent experiments ($n = 3$, mean ± SE; $^{*}p < 0.05$; $^{**}p < 0.01$). (E) NMD inhibitory effect of HTLV-1 infection is diminished by AZT treatment in HTLV-1 infected sHeLa cells by co-cultivation with MT-2 cells. NMD inhibition by HTLV-1 was abrogated in a dose-dependent manner by AZT treatment ($n = 6$, mean ± SD; $^{***}p < 0.001$).

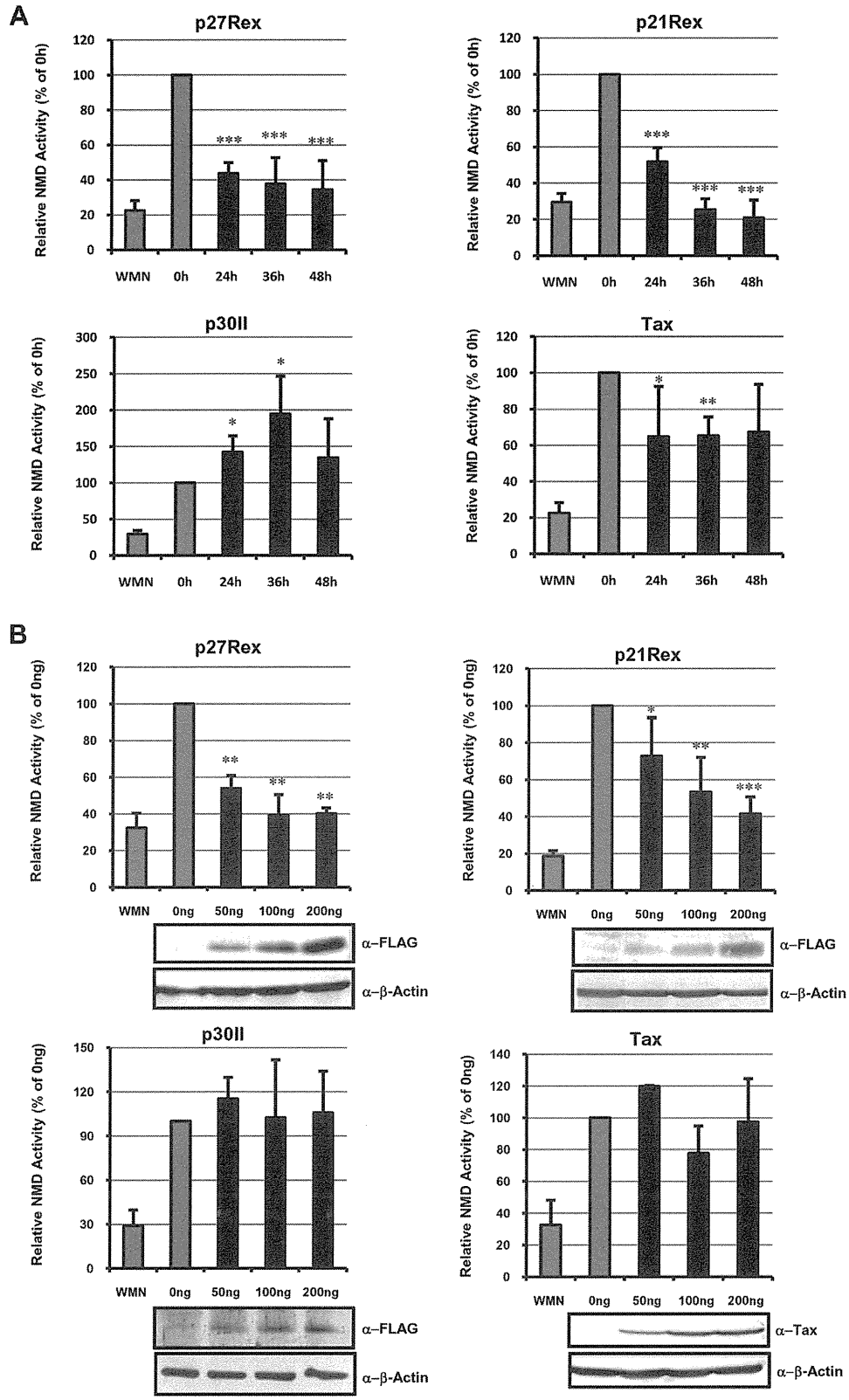

Fig. 4. HTLV-1 Rex is the key viral factor inhibiting NMD. (A) p27Rex and p21Rex inhibit NMD activity in a time-dependent manner, when 200 ng each of viral protein expression plasmid was transfected to sHeLa cells. Tax also demonstrated an NMD inhibitory effect but to a less significant level compared with p27Rex and p21Rex. A representative result from three independent experiments is shown ($n = 3$, mean ± SD; $^{*}p < 0.05$; $^{**}p < 0.01$; $^{***}p < 0.001$). (B) Both p27Rex and p21Rex suppressed NMD activity in a dose-dependent manner when 50–200 ng of viral protein expression plasmid was transfected to sHeLa cells. A representative result from three independent experiments is shown ($n = 3$, mean ± SD; $^{*}p < 0.05$; $^{**}p < 0.01$; $^{***}p < 0.001$).

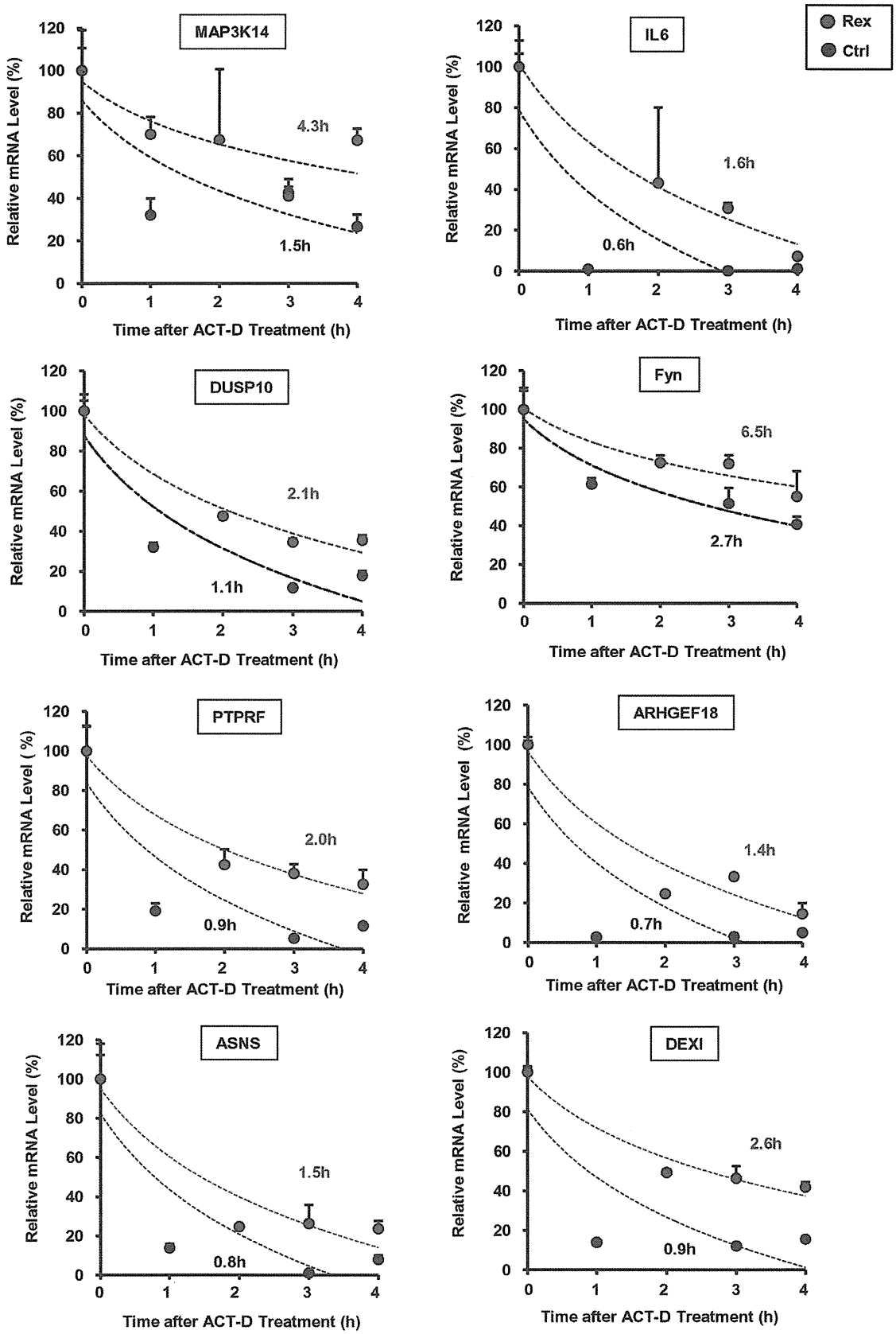

Fig. 5. Rex inhibits global NMD activity. The stability of NMD target mRNAs containing uORFs or 3′ UTR introns as NMD-inducing features [2] were measured in CEM-Rex and CEM-Ctrl. These mRNAs for NMD substrates were significantly stabilized in Rex-overexpressing cells, indicating that Rex represents a general block to global cellular NMD activity. Red circle: CEM-Rex; black circle: CEM-Ctrl. The indicated time is the half-life of tested mRNA calculated based on the regression curve (dashed line).

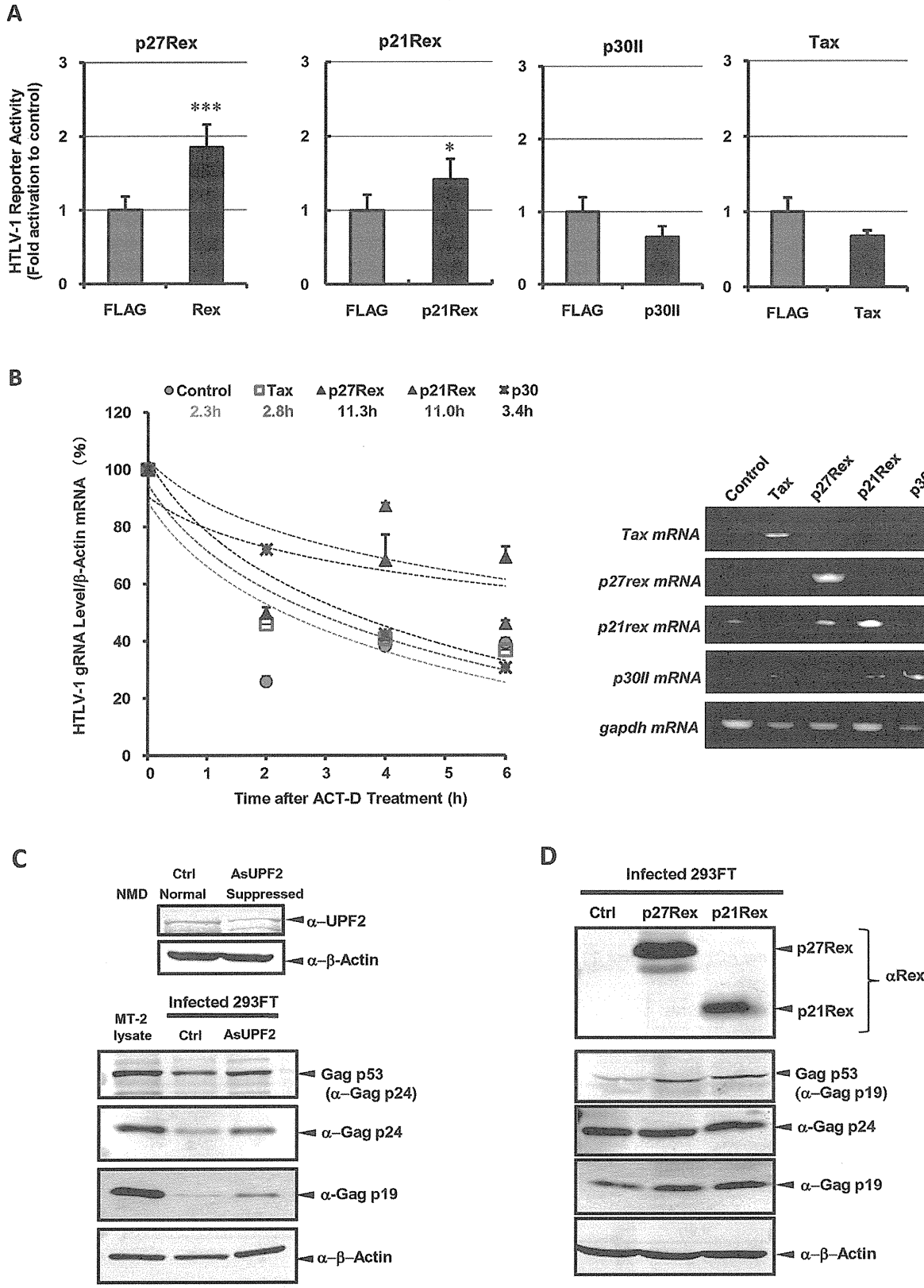

Fig. 6. Rex stabilizes HTLV-1 unspliced mRNA and enhances viral replication via NMD inhibition. (A) The effects of p27Rex, p21Rex, p30II, and Tax on HTLV-1 derived reporter activity in HeLa cells. The reporter activity was significantly increased by p27Rex and p21Rex but not by p30II and Tax ($n = 3–5$, mean ± SD; $^{*}p < 0.05$; $^{***}p < 0.001$). (B) The effect of HTLV-1 regulatory proteins p27Rex (red ▲), p21Rex (purple ▲), p30II (black×), Tax (blue□), and control (green●) on the stability of HTLV-1 genomic unspliced RNA in HTLV-1 infected HeLa cells by co-cultivation with MT-2 cells. HTLV-1 unspliced RNA in p27Rex-overexpressing cells was significantly stabilized (half-life = 11.3 h), followed by stabilization in p21Rex-overexpressing cells (half-life = 11.0 h) compared

to the Rex response element (RxRE) of viral transcripts and promotes selective nuclear export of viral genomic RNA [32,36]. P30II is also an RNA-binding protein that binds mainly to double-spliced *tax/rex* mRNA and reduces translation from this mRNA by retaining it to the nucleolus [37–39]. In a series of experiments testing the influence of these viral factors on NMD activity, only p27Rex and p21Rex displayed a robust time- and dose-dependent inhibition of NMD activity (Fig. 4). The most important and well-studied function of Rex is to promote nuclear export and enhance the stability of unspliced and singly spliced HTLV-1 mRNAs that encode viral structural proteins, by interacting with Rex Responsive Element (RxRE) situated at the 3′ end of all HTLV-1 mRNAs [18,19,40–42], and by engagement with the cellular nuclear export factor CRM1 [18,43,44]. The molecular mechanism of Rex in protection of unspliced viral RNA has not been fully clarified, however, partially explained by active export of mRNA from the nucleus, thereby escaping from the site of splicing. Nevertheless, the fate of viral RNA in the cytoplasm has not been methodically explored. From our data, we propose that Rex assists viral RNA transit within the cytoplasm and ensures efficient translation by subduing NMD and the host mRNA surveillance systems.

We demonstrated that the NMD activity of TL-Om1 cells was significantly suppressed (Fig. 3B), although these cells do not express any of viral proteins at detectable levels. The molecular mechanism of NMD inhibition in TL-Om1 cells is apparently different from that of Rex expressing cells, however, it can be conceived that disturbances of cellular homeostasis caused by HTLV-1 during the early stages of infection, including inhibition of NMD by Rex, might have been conserved after malignant transformation of the infected cells. To gain further insights into the mechanisms, comparative analyses of cell lines that were HTLV-1 immortalized in vitro, such as MT-2, and those derived from ATL and without Rex expression, such as TL-Om1, may provide valuable information as model cells in the early stages of infection and immortalization, and those in the later transformed phase, respectively.

During the completion of our study, Mocquet et al. [45] demonstrated that HTLV-1 Tax interacts with UPF1 and exerts an inhibitory effect on NMD activity. In the present study, Tax also consistently exhibited an inhibitory effect on NMD activity, but both p21Rex and p27Rex consistently outperformed Tax in our assays (Figs. 4 and 6A). Therefore, the studies described here specifically focused on the inhibition of NMD activity exerted by both Rex alleles. In our view, it is not surprising that retroviruses have evolved multiple and overlapping mechanisms to overcome the restrictive properties of NMD. This is especially relevant at early times of viral infection or alternatively, when the provirus is emerging from latency. Under such conditions, there may be insufficient Rex concentration to saturate the NMD pathway. Therefore, another mechanism that augments the NMD inhibitory activity of Rex, such as that presented by Tax, may be required to cooperatively incapacitate NMD. Significantly, recent studies have demonstrated that *tax/rex* mRNAs are the most abundant viral transcripts at early times of infection or following proviral reactivation, and that viral gene expression follows a two-phase pattern that is determined principally by Rex [46].

Our data are consistent with the view that increased luciferase activity of NMD-sensitive reporters by Rex was due to the suppression of overall cellular NMD activity but not due to RxRE-mediated nuclear export of reporter mRNAs by Rex. This is because (1) none of the NMD reporter mRNAs used in this study contain RxRE; (2) the amounts of unspliced and spliced forms of β-globin mRNA in nuclear and cytosolic fractions of the cells were not influenced by Rex expression (Fig. S3A); and (3) the insertion of RxRE after the β-globin fragment of the NMD reporter plasmids had no impact on the NMD inhibitory effect of Rex (Fig. S3B). The data that p21Rex, lacking NLS and RxRE-binding domain at the N-terminal region, is also capable of suppressing NMD strongly support the notion that NMD inhibition is genetically separable from the RxRE-binding function of Rex (Fig. 4). Indeed, we demonstrated that Rex stabilizes a series of NMD target mRNA with NMD-inducing features such as uORFs and 3′ UTR introns (Fig. 5), providing strong evidence that Rex blocks overall cellular NMD activity. On the other hand, it is widely accepted that NMD is involved in cellular homeostasis not only by eliminating PTC-containing aberrant mRNAs but also by controlling the levels of natural transcripts. Approximately 1–10% of eukaryotic transcripts are known to be targeted by NMD because of their potentially NMD-sensitive structures, i.e., PTCs encoded by alternative exons, introns in 3′ UTRs, or uORFs [2,47]. Thus, NMD dysfunction can lead to the destruction of cell homeostasis and may even trigger tumorigenesis [48]. Clearly, overall NMD inhibition by Rex is beneficial to HTLV-1 as a direct mechanism to enhance the stability of HTLV-1 genomic RNA. In contrast, it may perturb cellular gene expression and discrimination of aberrant mRNAs, which are critically regulated by NMD under normal conditions. Indeed, NMD targets many mRNAs, of which products participate in cell cycle regulation, T cell

with that in control cells (half-life = 2.3 h). In contrast, Tax and p30II did not significantly stabilize HTLV-1 unspliced RNA (half-lives = 2.8 and 3.4 h, respectively). The half-life was calculated based on the regression curve (dashed line) (n = 4, mean ± SE). The right side panel shows mRNAs levels of *tax*, *p27rex*, *p21rex*, and *p30ii* at 0 h measured by semi-quantitative RT-PCR in HTLV-1 infected cells expressing the indicated viral proteins, ectopically. (C) Expression of HTLV-1 structural proteins, Gag p53 (precursor), p24, and p19, in HTLV-1 infected 293FT cells co-cultured with MT-2 after NMD suppression by As-*upf2* mRNA overexpression to knockdown UPF2 protein expression (top panel). The expression levels of all Gag proteins, p53, p24, and p19, were significantly elevated in the 293FT cells after NMD suppression. (D) The influence of p27Rex and p21Rex on the expression of HTLV-1 Gag structural proteins, p53, p24, and p19, in HTLV-1 infected 293FT cells co-cultured with MT-2. The results showed that the expression levels of HTLV-1 Gag proteins, especially those of Gag p53 and p19, were significantly increased by p27Rex and p21Rex overexpression.

development, and inflammation [2]. The potential pleiotropic impact of Rex mediated through the NMD pathway represents an important and novel aspect of host–retrovirus interaction in viral leukemogenesis.

In conclusion, this study provides evidence that the host-encoded NMD pathway restricts viral RNA expression, thereby reducing HTLV-1. Furthermore, we demonstrated that a novel function for HTLV-1 Rex in inhibition of the host NMD machinery. Rex-mediated inhibition of NMD activity is pleiotropic and may affect both viral and cellular target RNA. Together with the data presented here, there is accumulating evidence of a dynamic interplay between the cellular NMD pathway and pathways for viral gene expression and replication. Clarifying underlying molecular mechanism in inhibition of NMD by Rex is essential to understand this new aspect of host–pathogen interaction. Finally we suggest that the NMD pathway may exert anti-viral effects on other RNA viruses and may participate generally in the innate immune response to viral pathogens. It is therefore likely that other viruses have evolved mechanisms to silence NMD activity during viral infection.

Acknowledgment

This work was supported by Grants-in-Aid for Scientific Research from the Ministry of Education, Culture, Sports, Science, and Technology of Japan, to TW (No. 19659241) and to KN (Nos. 22700863, 24501304).

Appendix A. Supplementary data

Supplementary data related to this article can be found at http://dx.doi.org/10.1016/j.micinf.2013.03.006.

References

[1] R.T. Hillman, R.E. Green, S.E. Brenner, An unappreciated role for RNA surveillance, Genome Biol. 5 (2004) R8.
[2] J.T. Mendell, N.A. Sharifi, J.L. Meyers, F. Martinez-Murillo, H.C. Dietz, Nonsense surveillance regulates expression of diverse classes of mammalian transcripts and mutes genomic noise, Nat. Genet. 36 (2004) 1073–1078.
[3] F.J. Iborra, A.E. Escargueil, K.Y. Kwek, A. Akoulitchev, P.R. Cook, Molecular cross-talk between the transcription, translation, and nonsense-mediated decay machineries, J. Cell Sci. 117 (2004) 899–906.
[4] L.E. Maquat, Nonsense-mediated mRNA decay: splicing, translation and mRNP dynamics, Nat. Rev. 5 (2004) 89–99.
[5] L. Balvay, M.L. Lastra, B. Sargueil, J. Darlix, T. Ohlmann, Translational control of retroviruses, Nat. Rev. 5 (2007) 128–140.
[6] N.J. McGlincy, C.W. Smith, Alternative splicing resulting in nonsense-mediated mRNA decay: what is the meaning of nonsense? Trends Biochem. Sci. 33 (2008) 385–393.
[7] E.P. Plant, P. Wang, J.L. Jacobs, J.D. Dinman, A programmed-1 ribosomal frameshift signal can function as a *cis*-acting mRNA destabilizing element, Nucleic Acids Res. 32 (2004) 784–790.
[8] A.L. Saltzman, Y.K. Kim, Q. Pan, M.M. Fagnani, L.E. Maquat, B.J. Blencowe, Regulation of multiple core spliceosomal proteins by alternative splicing-coupled nonsense-mediated mRNA decay, Mol. Cell Biol. 28 (2008) 4320–4330.
[9] C. Theis, J. Reeder, R. Giegerich, KnotInFrame: prediction of -1 ribosomal frameshift events, Nucleic Acids Res. 36 (2008) 6013–6020.
[10] A.M. Dickson, J. Wilusz, Strategies for viral RNA stability: live long and prosper, Trends Genet. 27 (2011) 286–293.
[11] S. Boelz, G. Neu-Yilik, N.H. Gehring, M.W. Hentze, A.E. Kulozik, A chemiluminescence-based reporter system to monitor nonsense-mediated mRNA decay, Biochem. Biophys. Res. Commun. 349 (2006) 186–191.
[12] T. Ohsugi, T. Kumasaka, T. Urano, Construction of a full-length human T cell leukemia virus type I genome from MT-2 cells containing multiple defective proviruses using overlapping polymerase chain reaction, Anal. Biochem. 329 (2004) 281–288.
[13] N.H. Gehring, G. Neu-Yilik, T.W. Schell, M. Hentze, A.E. Kulozik, Y14 and hUpf3b form an NMD-activating complex, Mol. Cell 11 (2003) 939–949.
[14] Y.K. Kim, L. Furic, L. DesGroseillers, L.E. Maquat, Mammalian staufen1 recruits Upf1 to specific mRNA 3_UTRs so as to elicit mRNA decay, Cell 120 (2005) 195–208.
[15] B. Lee, Y. Tanaka, H. Tozawa, Monoclonal antibody defining Tax1 protein of human T-cell leukemia virus type-I, Tohoku J. Exp. Med. 157 (1989) 1–11.
[16] Y. Tanaka, B. Lee, T. Inoi, H. Tozawa, N. Yamamoto, Y. Hinuma, Antigens related to three core proteins of HTLV-I (p24, p19 and p15) and their intracellular localizations, as defined by monoclonal antibodies, Int. J. Cancer 37 (1986) 35–42.
[17] J. Zhao, B.K. Sun, J.A. Erwin, J. Song, J.T. Lee, Polycomb proteins targeted by a short repeat RNA to the mouse X chromosome, Science 322 (2008) 750–756.
[18] M. Gröne, C. Koch, R. Grassmann, The HTLV-1 Rex protein induces nuclear accumulation of unspliced viral RNA by avoiding intron excision and degradation, Virology 218 (1996) 316–325.
[19] M. Hidaka, J. Inoue, M. Yoshida, M. Seiki, Post-transcriptional regulator (rex) of HTLV-1 initiates expression of viral structural proteins but suppresses expression of regulatory proteins, EMBO J. 7 (1988) 519–523.
[20] J. Inoue, M. Yoshida, M. Seiki, Transcriptional (p40x) and post-transcriptional (p27x-III) regulators are required for the expression and replication of human T-cell leukemia virus type I genes, Proc. Natl. Acad. Sci. U. S. A. 84 (1987) 3653–3657.
[21] A. Eulalio, I. Behm-Ansmant, E. Izaurralde, P-Bodies: at the crossroads of post-transcriptional pathways, Nat. Rev. 8 (2007) 9–22.
[22] T.M. Franks, G. Singh, J. Lykke-Andersen, UPF1 ATPase dependent mRNP disassembly is required for completion of nonsense-mediated mRNA decay, Cell 143 (2010) 938–950.
[23] O. Isken, L.E. Maquat, The multiple lives of NMD factors: balancing roles in gene and genome regulation, Nat. Rev. 9 (2008) 699–712.
[24] R. Parker, U. Sheth, P bodies and the control of mRNA translation and degradation, Mol. Cell 25 (2007) 635–646.
[25] J. Rehwinkel, I. Behm-Ansmant, D. Gatfield, E. Izaurralde, A crucial role for GW182 and the DCP1:DCP2 decapping complex in miRNA-mediated gene silencing, RNA 11 (2005) 1640–1647.
[26] U. Sheth, R. Parker, Targeting of aberrant mRNAs to cytoplasmic processing bodies, Cell 125 (2006) 1095–1109.
[27] L. Unterholzner, E. Izaurralde, SMG7 acts as a molecular link between mRNA surveillance and mRNA decay, Mol. Cell 16 (2004) 587–596.
[28] J.E. Weil, K.L. Beemon, A 3′ UTR sequence stabilizes termination codons in the unspliced RNA of Rous sarcoma virus, RNA 12 (2007) 102–110.
[29] E.G. Lee, D. Kuppers, M. Horn, J. Roy, C. May, M.L. Linial, A premature termination codon mutation at the C terminus of foamy virus *gag* downregulates the levels of spliced *pol* mRNA, J. Virol. 82 (2008) 1656–1664.
[30] L. Ajamian, L. Abrahamyan, M. Milev, P.V. Ivanov, A.E. Kulozik, N.H. Gehring, A.J. Mouland, Unexpected roles for UPF1 in HIV-1 RNA metabolism and translation, RNA 14 (2008) 914–927.
[31] J.R. Hogg, S.P. Goff, UPF1 senses 3′ UTR length to potentiate mRNA decay, Cell 143 (2010) 379–389.
[32] O.U. Susova, V.E. Gurtsevich, The role of region pX in the life cycle of HTLV-I and in carcinogenesis, Mol. Biol. 37 (2003) 334–344.
[33] G. Franchini, R. Fukumoto, J.R. Fullen, T-cell control by human T-cell leukemia/lymphoma virus type-1, Int. J. Hematol. 78 (2003) 280–296.
[34] M. Boxus, J.-C. Twizere, S. Legros, J.-F. Dewulf, R. Kettmann, L. Willems, The HTLV-1 Tax interactome, Retrovirology 5 (2008) 76.

[35] F. Kashanchi, J.N. Brady, Transcriptional and post-transcriptional gene regulation of HTLV-1, Oncogene 24 (2005) 5938–5951.
[36] I. Younis, P.L. Green, The human T-cell leukemia virus Rex protein, Front. Biosci. 10 (2005) 431–445.
[37] C. Nicot, M. Dundr, J.M. Johnson, J.R. Fullen, N. Alonzo, R. Fukumoto, G.L. Princler, D. Derse, T. Misteli, G. Franchini, HTLV-1-encoded p30II is a post-transcriptional negative regulator of viral replication, Nat. Med. 10 (2004) 197–201.
[38] U. Sinha-Datta, A. Datta, S. Ghorbel, M. Duc Dodon, C. Nicot, Human T-cell lymphotrophic virus type I Rex and p30 interactions govern the switch between virus latency and replication, J. Biol. Chem. 282 (2007) 14608–14615.
[39] H.H. Baydoun, M. Bellon, C. Nicot, HTLV-1 yin and yang: Rex and p30 master regulators of viral mRNA trafficking, AIDS Rev. 10 (2008) 195–204.
[40] Y.F. Ahmed, G.M. Gilmartin, S.M. Hanly, J.R. Nevins, W.C. Greene, Structure–function analyses of the HTLV-I Rex and HIV-1 Rev RNA response elements: insights into the mechanism of Rex and Rev action, Gene Develop. 4 (1990) 1014–1022.
[41] Y.F. Ahmed, G.M. Gilmartin, S.M. Hanly, J.R. Nevins, W.C. Greene, The HTLV-I Rex response element mediates a novel form of mRNA polyadenylation, Cell 64 (1991) 727–737.
[42] Y. Adachi, T. Nosaka, M. Hatanaka, Protein kinase inhibitor H-7 blocks accumulation of unspliced mRNA of human T-cell leukemia virus type I (HTLV-I), Biochem. Biophys. Res. Commun. 169 (1990) 469–475.
[43] Y. Hakata, T. Umemoto, S. Matsushita, H. Shida, Involvement of human CRM1 (exportin 1) in the export and multimerization of the Rex protein of human T-cell leukemia virus type 1, J. Virol. 72 (1998) 6602–6607.
[44] Y. Hakata, M. Yamada, Rat CRM1 is responsible for the poor activity of human t-cell leukemia virus type 1 Rex protein in rat cells, J. Virol. 75 (2001) 11515–11525.
[45] V. Mocquet, J. Neusiedler, F. Rende, D. Cluet, J.-P. Robin, J.-M. Terme, M. Duc Dodon, J. Wittmann, C. Morris, H.L. Hir, V. Ciminale, P. Jalinot, The human t-lymphotropic virus type 1 Tax protein inhibits nonsense-mediated mRNA decay by interacting with INT6/EIF3E and UPF1, J. Virol. 86 (2012) 7530–7543.
[46] F. Rende, I. Cavallari, A. Corradin, M. Silic-Benussi, F. Toulza, G.M. Toffolo, Y. Tanaka, S. Jacobson, G.P. Taylor, D.M. D'Agostino, C.R.M. Bangham, V. Ciminale, Kinetics and intracellular compartmentalization of HTLV-1 gene expression: nuclear retention of HBZ mRNAs, Blood 117 (2011) 4855–4859.
[47] P. Nicholson, H. Yepiskoposyan, S. Metze, R.Z. Orozco, N. Kleinschmidt, O. Mühlemann, Nonsense-mediated mRNA decay in human cells: mechanistic insights, functions beyond quality control and the double-life of NMD factors, Cell. Mol. Life Sci. 67 (2010) 677–700.
[48] L.B. Gardner, Nonsense-mediated RNA decay regulation by cellular stress: implications for tumorigenesis, Mol. Cancer Res. 8 (2010) 295–308.

AIDS RESEARCH AND HUMAN RETROVIRUSES
Volume 29, Number 5, 2013

DOI: 10.1089/aid.2012.0205

Altered Expression of Degranulation-Related Genes in CD8$^+$ T Cells in Human T Lymphotropic Virus Type I Infection

Tathiane M. Malta,[1,2] Israel T. Silva,[1] Daniel G. Pinheiro,[1] Anemarie R.D. Santos,[1] Mariana T. Pinto,[1,2] Rodrigo A. Panepucci,[1,3] Osvaldo M. Takayanagui,[3] Yuetsu Tanaka,[4] Dimas T. Covas,[1,3] and Simone Kashima[1,2]

Abstract

Human T lymphotropic virus type I (HTLV-1) is the etiological agent of HTLV-1-associated myelopathy/tropical spastic paraparesis (HAM/TSP). CD8$^+$ T cells may contribute to the protection or development of HAM/TSP. In this study we used SAGE methodology to screen for differentially expressed genes in CD8$^+$ T cells isolated from HTLV-1 asymptomatic carriers (HAC) and from HAM/TSP patients to identify genes involved in HAM/TSP development. SAGE analysis was conducted by pooling samples according to clinical status. The comparison of gene expression profiles between HAC and HAM/TSP libraries identified 285 differentially expressed tags. We focus on cytotoxicity and cytokine-related genes due to their potential biological role in HTLV-1 infection. Our results showed that patients with HAM/TSP have high expression levels of degranulation-related genes, namely GZMH and PRF1, and of the cytoskeletal adaptor PXN. We found that GZMB and ZAP70 were overexpressed in HTLV-infected patients compared to the noninfected group. We also detected that CCL5 was higher in the HAM/TSP group compared to the HAC and CT groups. Our findings showed that CD8$^+$ T cells of HAM/TSP patients have an inflammatory and active profile. PXN and ZAP70 overexpression in HTLV-1-infected patients was described for the first time here and reinforces this concept. However, although active and abundant, CD8$^+$ T cells are not able to completely eliminate infected cells and prevent the development of HAM/TSP and, moreover, these cells might contribute to the pathogenesis of the disease by migrating to the central nervous system (CNS). These results should be further tested with biological functional assays to increase our understanding on the role of these molecules in the development of HTLV-1-related diseases.

Introduction

It is estimated that 20 million people worldwide are infected with human T lymphotropic virus type I (HTLV-1),[1] the etiological agent of adult T cell leukemia/lymphoma (ATLL),[2,3] HTLV-1-associated myelopathy/tropical spastic paraparesis (HAM/TSP),[4,5] and several inflammatory diseases.[6–8] However, only 2–5% of infected individuals will develop ATLL or HAM/TSP, while most will remain asymptomatic throughout life.[9,10] The mechanisms that lead to the development of disease are not fully understood.

HAM/TSP is characterized by chronic and progressive inflammation of the central nervous system (CNS) in which the immune response appears to play an important role during disease development. Immune response is one of the factors that determine proviral load (PVL) and hence the risk of developing HAM/TSP.[11] Most genotypic studies on HTLV-1 show no association between genetic variants of the virus and the risk of developing HAM/TSP.[12,13] However, studies on the polymorphisms in genes related to the production of inflammatory interleukins and DC-sign receptors,[13–15] done in HTLV-1-infected individuals, have found an association between disease susceptibility and/or development. Additionally, the high PVL, the invasion of infected cells to other compartments, and the low efficiency of the host immune response are factors also related to HAM/TSP development.[12,16]

[1]National Institute of Science and Technology in Stem Cell and Cell Therapy, Center for Cell Therapy and Regional Blood Center, Blood Center of Ribeirão Preto, Ribeirão Preto, São Paulo, Brazil.
[2]Faculty of Pharmaceutical Sciences, University of São Paulo, Ribeirão Preto, São Paulo, Brazil.
[3]Faculty of Medicine, University of São Paulo, Ribeirão Preto, São Paulo, Brazil.
[4]Department of Immunology, Graduate School of Medicine, University of the Ryukyus, Nishihara, Okinawa, Japan.

In fact, during HTLV-1 infection immune cells are strongly activated, mainly $CD4^+$ and $CD8^+$ T cells.[17,18] This increased immune response may contribute to tissue damage, as observed in the CNS of subjects who develop HAM/TSP.[19] It is unclear whether HTLV-1-specific $CD8^+$ T cells are responsible for protecting against HAM/TSP by controlling PVL or they are the cause of the inflammatory disease themselves.[20] Nevertheless, these two mechanisms are not mutually exclusive.

As the immune response against HTLV-1 is regulated by many genes, differences in gene expression profiles of $CD8^+$ T cells may contribute to the protection or development of HAM/TSP. Here we looked for differentially expressed genes in $CD8^+$ T cells isolated from asymptomatic HTLV-1-infected individuals and individuals with HAM/TSP, in an attempt to identify genes involved in the development of HAM/TSP. A better knowledge of the molecular mechanisms involved in HTLV-1 infection may provide a better understanding of the regulatory network related to HTLV-1-associated diseases.

Materials and Methods

Patients and controls

HTLV-1 patients belong to the positive serology profile of blood donors of the Regional Blood Center of Ribeirão Preto, São Paulo, Brazil and of patients from the Neurology Department of the Clinical Hospital of the Faculty of Medicine of the University of São Paulo, Ribeirão Preto, Brazil. The diagnosis of HTLV-1 was established by antibody screening of serum/plasma samples using an enzyme immunoassay (rp21e-enhanced EIA; Cambridge Biotech), followed by in house polymerase chain reaction (PCR) confirmation for *tax* and LTR.[21] The study was approved by the Institutional Ethics Committee (process number 3083/2007) and all patients signed an informed consent before enrollment. A total of 40 ml of peripheral blood was obtained from HTLV-1 patients and healthy volunteers. A total of 83 samples were collected. The subjects were divided into three groups: (1) the control group (CT) composed by 40 non-HTLV-1-infected individuals; (2) the asymptomatic group (HAC) composed of 24 HTLV-1-asymptomatic carriers; (3) and the HAM/TSP group (HAM/TSP) with 19 patients. All HTLV-1-seropositive individuals were evaluated for clinical status according to the criteria previously described for ATLL and HAM/TSP.[22] None of the HTLV-1-seropositive individuals showed positive serology for other relevant blood-borne pathogens including hepatitis B virus, hepatitis C virus, human immunodeficiency virus, HTLV-2, Chagas disease, and syphilis. Individuals included in the control group who were blood donors also showed negative serology for these pathogens. Individuals who were not blood donors were screened for HTLV-1 infection and we applied an oral questionnaire in order to search for other infections and for any drug treatment. The individuals who reported any infection or antiinflammatory treatment were excluded from the study. All individuals were evaluated for white blood cell (WBC) count and $CD4^+$ and $CD8^+$ T cell counts. The mean age was around 42.0 (range from 20 to 71) and 55.0 (range from 34 to 75) years old for the HAC and HAM/TSP groups, respectively. Of the HAM/TSP group 84.2% was composed of infected females, whereas 54.2% of the HAC group was composed of females. Of the CT group 75% was composed of women and the mean age was 43.2 years old (range from 22 to 76). The sex and age distribution of the sample groups are shown in Table 1.

Proviral load

The white cell layer was isolated by centrifugation at $900 \times g$ for 10 min at 4°C and transferred to sterile 15-ml polypropylene tubes. DNA was extracted from the buffy coat using a Super Quick Gene DNA Isolation kit (Analytical Genetic Testing Center, Denver, CO). After extraction, HTLV-1 PVL was determined by the quantitative PCR method using ABI Prism 7500 (Applied Biosystems) with 200 ng genomic DNA (roughly equivalent to 10^5 cells).

The reaction mixture was prepared using TaqMan Universal PCR Master Mix (Applied Biosystems) technology to amplify HTLV-1 *tax* and human actin beta (ACTB) genes. The primer set for the HTLV-I *tax* region was 5′-CGG ATA CCC IGT CTA CGT GTT T-3′ and 5′-CTG AGC IGA IAA CGC GTC CA-3′ and the TaqMan fluorescent probe for the *tax* gene was 5′-ATC ACC TGG GAC CCC ATC GAT GGA-3′.[23] To amplify the ACTB region we used the TaqMan Gene Expression Assays–Hs03023880_g1 (Applied Biosystems). The PCR conditions for *tax* amplification were 6.25 μl of the TaqMan Universal PCR Master Mix, 5 μM of each primer, and 5 μM of probe (Applied Biosystems). For ACTB amplification the reaction conditions were 5.0 μl of TaqMan Universal PCR Master Mix and 0.5 μl of probe. The thermal cycler settings were 50°C for 2 min, 95°C for 10 min, and 40 cycles at 95°C for 15 s and 60°C for 1 min. DNA standards were extracted from the MT-2 cell line to make a standard curve. Based on the standard curve created by six concentrations of template (10^1 to 10^6 copies), the concentrations of unknown samples were determined. The amount of HTLV-1 proviral DNA was calculated by the following formula: copy number of HTLV-1 *tax* per 1×10^5 PBMCs = [(copy number of *tax*)/(copy number of ACTB)] $\times 2 \times 10^5$. All samples were duplicated.

$CD8^+$ T cell separation

Peripheral blood mononuclear cells (PBMCs) were separated from whole blood using the Ficoll-Paque PLUS density gradient (GE Healthcare Bio-Sciences AB, Uppsala, Sweden) and stored in fetal bovine serum (FBS) containing 10% dimethyl sulfoxide (DMSO) at N_2 for posterior stained and flow cytometry analysis. $CD8^+$ T cells were isolated using anti-CD8 Ab-coated microbeads by passing PBMCs through a magnetic cell separation system (MACS; Miltenyi Biotec, Bergish Glabach, Germany) with column type LS. The positively selected cells were confirmed as being $CD8^+$ T cells by flow cytometry analysis (FACSCalibur, Becton & Dickinson, San Jose, CA).

Tax expression

PBMCs isolated from 14 HAC and 11 HAM/TSP patients were stained with anti-Tax and analyzed by flow cytometry to quantify the amount of cells that are capable of expressing Tax. PBMCs were cultured in RPMI-1640 medium (Sigma-Aldrich) supplemented with 10% of FBS, 2 mmol/liter glutamine, 100 IU/ml penicillin, 100 μg/ml streptomycin, and 20 nmol/liter concanamycin A (CMA) (Sigma-Aldrich) for 14 h. Harvested cells were washed with phosphate-buffered saline (PBS) and stained with antihuman-CD4-phycoerythrin

Table 1. Descriptive Characteristics of the Control Group, Human T Lymphotropic Virus Type I-Asymptomatic Carriers, and Human T Lymphotropic Virus Type I-Associated Myelopathy/Tropical Spastic Paraparesis Patients According to Clinical Status, Age, Gender, Proviral Load, White Blood Cell Count, and CD4/CD8 Ratio

	Mean age	Gender (%)		Proviral load mean (copy number/10^5 cells)	White blood cell count (cells/mm^3)	CD4/CD8 ratio (mean values)
		F	M			
CT ($n=40$)	43.2	75.0	25.0	—	7,291	2.06
HAC ($n=24$)	42.0	54.2	45.8	173.5	6,782	1.95
HAM/TSP ($n=19$)	55.0	84.2	15.8	1,075.1	7,272	2.34

F, female; M, male; CT, control group; HAC, HTLV-1-asymptomatic carriers; HAM/TSP, HTLV-1-associated myelopathy/tropical spastic paraparesis.

(PE), antihuman-CD8-PE, and anti-human-CD3-Peridinin Chlorophyll Protein (PerCP) (Becton & Dickinson). Cells were fixed in PBS 1×containing 4% (v/v) paraformaldehyde (Sigma-Aldrich) for 20 min and resuspended in PBS. Fixed cells were washed with PBS containing 4% normal goat serum (Sigma-Aldrich) and permeabilized with PBS containing 0.1% (v/v) Triton X-100 (Sigma-Aldrich) for 7 min at room temperature. Permeabilized cells were washed, resuspended in PBS/4% normal goat serum containing an anti-Tax MAb (Lt-4),[24] and incubated for 30 min. After washing, Alexa Fluor 488-conjugated antimouse IgG3 serum (Invitrogen, Carlsbad, CA) was used as the second antibody for labeling anti-Tax. Finally, the cells were washed twice, analyzed by flow cytometry (FACSCalibur, Becton & Dickinson), and the proportion of $CD8^+$ T cells positive for Tax protein was estimated, indicating the number of $CD8^+$ T cells infected by HTLV-1 capable of expressing the Tax protein.

SAGE procedure

Analysis of the SAGE global gene expression profile was conducted by pooling samples according to clinical status into the HAC and HAM/TSP groups. Each pool was composed by equal amounts of RNA of four individuals whose $CD8^+$ T cells purity was above 80%. Thus, the HAC group was composed of HAC 01, HAC 09, HAC 10, and HAC 11 samples. The HAM/TSP group was composed of HAM/TSP 01, HAM/TSP 05, HAM/TSP 08, and HAM/TSP 09 (Table 2). Total RNA was isolated from $CD8^+$ T cells using TRIzol LS Reagent (Invitrogen) according to the manufacturer's instructions. Twenty-five micrograms of total RNA was used for the SAGE procedure carrying out the I-SAGE Kit (Invitrogen) based on the original SAGE.[25] Amplified inserts were sequenced with forward M13 primer in a MegaBACE 1000 sequencer and the DYEnamic ET Dye Terminator Sequencing Kit (Amersham Biosciences, Piscataway, NJ).

SAGE analysis

HAC and HAM/TSP SAGE tags were extracted from concatamer sequences and analyzed by SAGE 2000 software, version 4.5 (www.sagenet.org), using default parameters. Tag-to-gene assignments were performed based on the CGAP SAGE Genie database ("Hs_short.best_gene" at http://cgap.nci.nih.gov/SAGE). SAGE libraries from the HAC and HAM/TSP groups can be found at the NCBI GEO database numbers GSM641893 and GSM641894, respectively. To compare the gene expression among libraries, the number of tags was normalized to a total count of 300,000 tags. Tags identified as contaminants or technical artifacts were filtered using S3T analysis.[26] The Audic and Claverie significance test[27] and a Fold-Change (FC) criterion were used to identify differently expressed genes (DEG) between libraries (p value <0.01 and $FC>2$). We also estimated the false discovery

Table 2. Descriptive Characteristics of Human T Lymphotropic Virus Type I-Asymptomatic Carriers and Human T Lymphotropic Virus Type I-Associated Myelopathy/Tropical Spastic Paraparesis Patients Included in SAGE Libraries, According to Clinical Status, Gender, Age, Proviral Load, White Blood Cell Count, CD4/CD8 Ratio, and Purity of $CD8^+$ T Cells

Clinical status	Gender	Age (years)	Proviral load (copy number/10^5 cells)	White blood cell count (cells/mm^3)	CD4/CD8 (ratio)	Purity $CD8^+$
HAC 01	F	52	17.7	7,400	1,224/697 (1.76)	82.26%
HAC 09	F	47	50.4	5,900	676/512 (1.32)	90.57%
HAC 10	F	21	15.3	7,100	875/529 (1.65)	91.19%
HAC 11	M	38	321.6	6,400	1,299/538 (2.41)	90.99%
Mean		39.5	101.2	6,700	(1.79)	
HAM/TSP 01	F	34	300.8	7,600	717/378 (1.90)	87.93%
HAM/TSP 05	F	53	888.1	7,100	2,497/1,001 (2.49)	84.56%
HAM/TSP 08	M	55	1,091.4	8,200	ND	98.90%
HAM/TSP 09	M	55	995.3	3,700	468/355 (1.32)	89.86%
Mean		49.3	818.9	6,650	(1.90)	

F, female; M, male; HAC, HTLV-1-asymptomatic carriers; HAM/TSP, HTLV-1-associated myelopathy/tropical spastic paraparesis; ND, not determined.

rate (FDR) in order to evaluate the genes with differential expression.[28] The set of DEG was selected for functional analysis, using annotation databases from Gene Ontology, KEGG, and BioCarta, providing, respectively, the identification of biological processes and interactions of genes into pathways. The DEG was also submitted to Ingenuity Pathway Analysis (IPA) (Ingenuity Systems, www.ingenuity .com). For gene expression analysis, we also used public SAGE libraries from leukocytes obtained from venous blood of normal healthy volunteers[29] (accession number GSE5833).

Real-time quantitative PCR

For qRT-PCR analysis, we studied a total of 55 samples, including the eight samples used to prepare SAGE libraries. Of the total, 24 were CT individuals, 17 were HAC, and 14 had HAM/TSP.

The RNA was reverse transcribed using a High Capacity cDNA Reverse Transcription Kit (Applied Biosystems). Real-time quantitative PCR was conducted in the cDNA of 55 individuals (unpooled) and was performed in 7,500 Real-Time PCR System (Applied Biosystems) using TaqMan Gene Expression Assays (Applied Biosystems) as recommended by the manufacturer. Primers (Applied Biosystems) for the following functionally diverse set of genes were used: perforin 1 (PRF1) (Hs00169473_m1), granzyme B (GZMB) (Hs0018051_m1), granzyme H (GZMH) (Hs00277212_m1), chemokine (C–C motif) ligand 5 (CCL5) (Hs00174575_m1), zeta-chain (TCR)-associated protein kinase 70 kDa (ZAP70) (Hs00896347_m1), and paxillin (PXN) (Hs01104424_m1). The amount of mRNA for each sample was normalized using the geometric average of the two housekeeping genes GAPDH (4310884-E) and RPL13A (185720330-7).[30] All the reactions were duplicated and PCR amplification efficiency was established for all genes and ranged from 0.9 to 1.1. The relative expression levels were calculated using the $2^{-\Delta\Delta Ct}$ method[31] and the median of the CT group was used as the calibrator.

Quantitative flow cytometry analysis

PBMCs were analyzed by quantitative flow cytometry for PRF1 and GZMB. Frozen PBMCs were used for intracellular staining of PRF1 and GZMB. A total of nine uninfected individuals, 15 and 14 patients from the HAC and HAM/TSP groups, respectively, were analyzed. Samples were thawed and washed with PBS and stained with antihuman-CD8-FITC or antihuman-CD8-PE, and with antihuman-CD3-PerCP (Becton & Dickinson). Cells were fixed in PBS containing 4% (v/v) paraformaldehyde (Sigma-Aldrich) and permeabilized with PBS containing 0.1% (v/v) Triton X-100 (Sigma-Aldrich). After washing, the cells were incubated with antihuman-PRF1-clone δG9 anti-PRF1-PE or anti-GZMB-FITC (Becton & Dickinson). Finally, the cells were washed and analyzed by flow cytometry (FACSCalibur, Becton & Dickinson). The mean fluorescence intensity (MFI) was determined, indicating the protein expression level.

Statistical analyses

The statistical analyses to compare the differences in PVL between the HAC and HAM/TSP groups were performed using the Mann–Whitney test. The Mann–Whitney test was also used to evaluate the differences in gene expression quantification between the two groups. Data related to expression levels among three groups were compared by ANOVA followed by Tukey post hoc analyses. To draw correlations between PVL and gene expression we used the nonparametric Spearman test. The statistical analyses were performed using SPSS software version 14. Values of p lower than 0.05 were considered statistically significant.

Results

Epidemiological and clinical features of HTLV-1-infected patients

A total of 83 individuals were tested; of them, 40 were CT individuals, 24 were HAC, and 19 had HAM/TSP. The values of WBC ranged from 2,800 to 12,500 cells/mm^3 but the mean value was similar among groups (Table 1). Nine samples (CT 03, CT 07, CT 08, CT 17, HAC 20, HAM/TSP 03, HAM/TSP 06, HAM/TSP 09, and HAM/TSP 15) showed a WBC count below the reference value whereas five samples (CT 05, CT 22, CT 39, HAM/TSP 12, and HAM/TSP 17) had higher values. For CD4$^+$ and CD8$^+$ count, the values were similar among groups (Table 1), ranging from 1.02 to 4.94. Three individuals (CT 16, HAC 15, and HAM/TSP 11) showed a CD4$^+$/CD8$^+$ ratio below 1.2. The PVL in the HAM/TSP group was six times higher (mean 1,075.1 copy number/10^5 cells) than in the HAC group (mean 173.5 copy number/10^5 cells) ($p < 0.05$) (Table 1).

The proportion of CD8$^+$ T cells infected by HTLV-1, evidenced by the Tax protein expression, was 2.2 times higher in

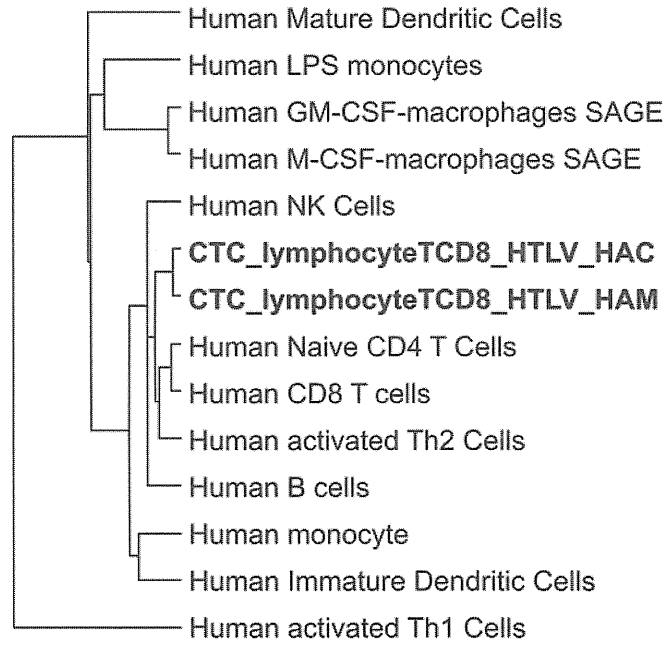

FIG. 1. Hierarchical clustering of leukocytes, dendritic cells, macrophages, and CD8$^+$ T cells isolated from human T lymphotropic virus type I (HTLV-1)-infected individuals. Briefly, a dendrogram was generated by pairwise average linkage (Euclidean distance) using Cluster 3.0 software. Myeloid and lymphoid cells were differentially clustering. CD8$^+$ T cell libraries derived from HTLV-1-infected individuals were grouped together in the lymphoid cluster.

the HAM/TSP group (1.607% mean value) compared to the HAC group (0.731% mean value) ($p=0.0294$).

SAGE library analysis

To access the identity of $CD8^+$ T cell libraries, we used hierarchical cluster analysis to compare the gene expression profile of our libraries with data from libraries of different leukocyte types. The dendrogram revealed that lymphoid and myeloid cells clustered separately. Notably, $CD8^+$ T cell libraries derived from HTLV-1-infected individuals were grouped together in the lymphoid cluster as shown in Fig. 1, indicating similarity in the gene expression patterns with lymphoid cells. HAC and HAM/TSP libraries also showed a tight correspondence, branching together.

A total of 62,432 and 60,620 tags were sequenced from HAC and HAM/TSP libraries, respectively. These tags yielded 12,262 and 13,025 unique tags mapped to known genes. Most identified and mapped tags (60%) appeared only once. Both libraries showed a large number of ribosomal protein tags. Supplementary Tables S1 and S2 (Supplementary Data are available online at www.liebertpub.com/aid) list the 50 most abundant tags (ribosomal tags were excluded) found in the HAC and HAM/TSP libraries, respectively. The most abundant tag identified in HAC and HAM/TSP libraries was the heterogeneous nuclear ribonucleoprotein A1 pseudogene 5 (HNRPA1P5).

Gene expression patterns observed in HAC versus HAM/TSP groups

We used SAGE libraries of pooled HAC and HAM/TSP $CD8^+$ T cells to screen for differentially expressed pathways involved in HAM/TSP development. Comparison of gene expression profiles between the HAC and HAM/TSP groups showed 285 differentially expressed tags. Tables 3 and 4 show the top 20 increased tag-associated transcripts in the HAC and in the HAM/TSP libraries, respectively. Of the 285 deregulated tags observed between HAC and HAM/TSP, 174 were overexpressed in the HAM/TSP group. To investigate the role of those differentially expressed tag-associated genes they were classified according to their biological function. We performed Ingenuity Pathways Analysis, which resulted in the annotation of the following most represented functional categories: apoptosis, cytolysis, cytotoxicity, cellular development, growth and proliferation, immunological and neurological diseases, inflammatory response, and diseases and infection. Additionally, we classified the differentially expressed genes into a number of functional categories according to Gene Ontology terms of interest (Table 5) to search for genes involved in HAM/TSP development. We found molecules related to immune response, such as zeta-chain (TCR)-associated protein kinase 70 kDa (ZAP70), leukocystatin (CST7), and linker for activation of T cells (LAT); apoptosis,

Table 3. Top 20 Increased Transcripts Expressed in the Human T Lymphotropic Virus Type I-Asymptomatic Carriers Library

Tag	*Symbol*	*Description*	*Normalized frequencies*		*FC*	p *value* ≤ *0.05*	*FDR*
			HAM/TSP	*HAC*			
CTGATCTGTG	HLA-B	Major histocompatibility complex, class I, B	0	54	54.0	Yes	0.00
AGCTGCAATC	EEF1G	Eukaryotic translation elongation factor 1 gamma	1	17	17.0	Yes	0.00
AATCCAGGAG	DDOST	Dolichyl-diphosphooligosaccharide-protein glycosyltransferase	1	16	16.0	Yes	0.00
CTGGCGCGAG	ARHGDIB	Rho GDP dissociation inhibitor (GDI) beta	4	57	14.3	Yes	0.00
CTGAGACGAA	BTF3	Basic transcription factor 3	0	14	14.0	Yes	0.00
TGTGGGAACC	SMAP1L	Stromal membrane-associated protein 1-like	0	12	12.0	Yes	0.00
ATCCGCAAGA	ACO1	Aconitase 1, soluble	1	12	12.0	Yes	0.00
GAATTTGTGT	EFCAB5	EF-hand calcium binding domain 5	1	12	12.0	Yes	0.00
GAGCAGGAGC	DIS3L2	DIS3 mitotic control homolog (*S. cerevisiae*)-like 2	1	12	12.0	Yes	0.00
GCCAAGGGGC	OGDH	Oxoglutarate (alpha-ketoglutarate) dehydrogenase (lipoamide)	1	12	12.0	Yes	0.00
TAGAAAAATA	GPI	Glucose phosphate isomerase	1	12	12.0	Yes	0.00
TGTTCCACTC	ENTPD6	Ectonucleoside triphosphate diphosphohydrolase 6 (putative function)	1	12	12.0	Yes	0.00
TTGAGCCAGC	KHSRP	KH-type splicing regulatory protein (FUSE binding protein 2)	1	12	12.0	Yes	0.00
GGGCCCCGCA	PMPCA	Peptidase (mitochondrial processing) alpha	0	11	11.0	Yes	0.00
GTGGTGTACG	RBM3	RNA binding motif (RNP1, RRM) protein 3	1	11	11.0	Yes	0.00
GTTCTCCCAC	SEC61A1	Sec61 alpha 1 subunit (*S. cerevisiae*)	1	11	11.0	Yes	0.00
TGGGCTGGGG	ADFP	Adipose differentiation-related protein	1	11	11.0	Yes	0.00
AAGATCAAGA	ACTA1	Actin, alpha 1, skeletal muscle	1	11	11.0	Yes	0.00
CTTGCCTGAA	BIN1	Bridging integrator 1	3	27	9.0	Yes	0.00
GGGGCTGGGG	EGLN2	Egl nine homolog 2 (*C. elegans*)	4	35	8.8	Yes	0.00
CTGACTTGTG	HLA-B	Major histocompatibility complex, class I, B	21	156	7.4	Yes	0.00

HAC, HTLV-1-asymptomatic carriers; HAM/TSP, HTLV-1-associated myelopathy/tropical spastic paraparesis; FC, fold change; FDR, false discovery rate. The tag sequence represents the 10-bp SAGE tag. Normalized frequencies were obtained using SAGE software by calculating the total number of 300,000.

TABLE 4. TOP 20 INCREASED TRANSCRIPTS EXPRESSED IN THE HUMAN T LYMPHOTROPIC VIRUS TYPE I-ASSOCIATED MYELOPATHY/TROPICAL SPASTIC PARAPARESIS LIBRARY

Tag	Symbol	Description	Normalized frequencies		FC	p value ≤ 0.05	FDR
			HAM/TSP	HAC			
CGAGGGGCCA	ACTN4	Actinin, alpha 4	18	1	18.0	Yes	0.00
GAAGCAATAA	ST3GAL3	ST3 beta-galactoside alpha-2,3-sialyltransferase 3	16	0	16.0	Yes	0.00
AGTCGGGAGC	HNRPK	Heterogeneous nuclear ribonucleoprotein K	14	1	14.0	Yes	0.00
CGGCCTCACC	TTYH2	Tweety homolog 2 (*Drosophila*)	14	0	14.0	Yes	0.00
GCAGGGTACA	KIAA1949	KIAA1949	14	0	14.0	Yes	0.00
TCTGAAGTCA	ID2	Inhibitor of DNA binding 2, dominant negative helix-loop-helix protein	14	0	14.0	Yes	0.00
TGTAAGTCTG	KHDRBS1	KH domain containing, RNA binding, signal transduction associated 1	14	0	14.0	Yes	0.00
CAAAAAAAAA	OCIAD1	OCIA domain containing 1	13	1	13.0	Yes	0.00
GGCCAGCAAT	GLIPR1	GLI pathogenesis-related 1 (glioma)	13	1	13.0	Yes	0.00
GCGTCCTGCC	LAT	Linker for activation of T cells	13	0	13.0	Yes	0.00
GCTAAAAAAA	FBF1	Fas (TNFRSF6) binding factor 1	13	0	13.0	Yes	0.00
TCTGCTAAAG	HMGB1	High-mobility group box 1	13	0	13.0	Yes	0.00
AATGCTGGCA	DNAJB6	DnaJ (Hsp40) homolog, subfamily B, member 6	11	1	11.0	Yes	0.00
ACCCTCTTCC	HLA-A	Major histocompatibility complex, class I, A	11	1	11.0	Yes	0.00
CTGGCCATCG	EHBP1L1	EH domain binding protein 1-like 1	11	1	11.0	Yes	0.00
GAGCGGGATC	SFRS1	Splicing factor, arginine/serine-rich 1 (splicing factor 2, alternate splicing factor)	11	1	11.0	Yes	0.00
GGGGGCCCCG	YIF1A	Yip1 interacting factor homolog A (*S. cerevisiae*)	11	1	11.0	Yes	0.00
AGATGAGATG	KLF6	Kruppel-like factor 6	11	0	11.0	Yes	0.00
GGGAATCAAA	CNO	Cappuccino homolog (mouse)	11	0	11.0	Yes	0.00
GTAGCAGGTG	M6PRBP1	Mannose-6-phosphate receptor binding protein 1	11	0	11.0	Yes	0.00

HAC, HTLV-1-asymptomatic carriers; HAM/TSP, HTLV-1-associated myelopathy/tropical spastic paraparesis; FC, fold change; FDR, false discovery rate. The tag sequence represents the 10-bp SAGE tag. Normalized frequencies were obtained using SAGE software by calculating the total number of 300,000.

such as granzyme H (GZMH), integrin beta 2 (ITGB2), and programmed cell death 4 (PDCD4); and inflammatory response, such as chemokine (C–C motif) ligand 5 (CCL5) and natural cytotoxicity triggering receptor 3 (NCR3), among others (Table 5).

Gene expression patterns observed in CT versus HTLV-1-infected groups (HAC or HAM/TSP)

We searched for differentially expressed tags between a public library of CD8+ T cells from normal healthy volunteers (CT) and HAC and also between CT and HAM/TSP in order to identify genes deregulated in HTLV-1 infection. Although this comparison has some drawbacks due to methodological and ethnical differences among samples, we could identify 899 differentially expressed tags from the comparison between CT and HAC, whereas CT and HAM/TSP revealed 855. From these tags we determined that many cytokine-related genes including chemokine (C–X–C motif) receptor 4 (CXCR4), interleukin 8 (IL-8), chemokine (C–C motif) ligand 20 (CCL20), and chemokine (C–C motif) receptor 7 (CCR7) were decreased in HTLV-1-infected groups (HAC and HAM/TSP), whereas IL-23, alpha (IL23A), lymphotoxin beta (LTB), IL-24, and CCL5 expressions were increased, when compared to the CT library.

Genes related to cytotoxicity were also identified as differentially expressed between CT and HTLV-1-infected libraries. For example, GZMH and granzyme A (GZMA) have a higher expression in HTLV-1-infected individuals than in the CT group.

Expression levels of cytotoxicity and cytokines genes were different between HAC and HAM/TSP patients

To further investigate the involvement of specific genes in HTLV-1 infection based on fold change in SAGE libraries and on their biological function, we selected the CCL5, GZMH, and ZAP70 genes to assess their gene expression levels by real time PCR in 55 samples. We also tested the cytolytic genes granzyme B (GZMB) and PRF1 and the cytoskeletal adaptor paxillin (PXN) to better explore their associated pathways.

In SAGE libraries, CCL5 was 3.5 times higher, GZMH was 2 times higher, and ZAP70 was 5.8 times higher in the HAM/TSP group than in HAC (Table 5). When we compared the expression levels of GZMB, PRF1, and PXN between the HAC and HAM/TSP libraries, we found an expression ratio lower than 2.0.

Relative quantification of CCL5 and GZMH by qRT-PCR corroborated SAGE data showing that their expression levels were significantly higher in the HAM/TSP than in the HAC group and also than in the CT group (Fig. 2A and B). When we tested ZAP70 by qRT-PCR we found a different result from SAGE, since no difference was observed between the HAC and HAM/TSP groups. Interestingly, we found that all infected patients (HAC + HAM/TSP) showed a significantly higher expression level of ZAP70 than the CT group (Fig. 2E). Expression of the cytotoxicity gene PRF1 was significantly higher in the HAM/TSP group than in the CT group (Fig. 2C). Analyzing gene expression of PXN by qRT-PCR, we found a significant increase in the HAM/TSP group compared to the CT group and also compared to the HAC groups (Fig. 2D).

TABLE 5. COMPARISON OF GENES DIFFERENTIALLY EXPRESSED BETWEEN HUMAN T LYMPHOTROPIC VIRUS TYPE I-ASYMPTOMATIC CARRIERS AND HUMAN T LYMPHOTROPIC VIRUS TYPE I-ASSOCIATED MYELOPATHY/TROPICAL SPASTIC PARAPARESIS $CD8^+$ T CELL LIBRARIES FOR SELECTED TERMS OF GENE ONTOLOGY

		Normalized frequencies			
Tag	*FC*	*HAM/TSP*	*HAC*	*Gene symbol*	*Description*
Immune response					
CTGATCTGTG	54.0	1	54	HLA-C	Major histocompatibility complex, class I, C
CTGGCGCGAG	14.3	4	57	ARHGDIB	Rho GDP dissociation inhibitor (GDI) beta
CTGACTTGTG	7.4	21	156	HLA-C	Major histocompatibility complex, class I, C
TGACCCACCA	8.0	1	8	HLA-C	Major histocompatibility complex, class I, C
TGGGAGCTCA	8.0	1	8	NCR3	Natural cytotoxicity triggering receptor 3
CTGACCTGTG	−2.0	483	240	HLA-C	Major histocompatibility complex, class I, C
GGCTCCTCGA	−2.1	19	9	TAPBP	TAP binding protein (tapasin)
GCTTAATGCT	−2.2	24	11	CD8B	CD8b molecule
GTAGCACCTC	−2.3	69	30	CST7	Cystatin F (leukocystatin)
TTCCCTTCTT	−2.4	26	11	HLA-DPB1	Major histocompatibility complex, class II, DP beta 1
CCACTACACT	−3.5	14	4	TNFSF10	Tumor necrosis factor (ligand) superfamily, member 10
CCTCTAGAGG	−3.5	14	4	CCL5	Chemokine (C–C motif) ligand 5
GCTGAACGCG	−3.0	9	3	CEBPB	CCAAT/enhancer binding protein (C/EBP), beta
AGGGGCTGCC	−4.8	19	4	HLA-C	Major histocompatibility complex, class I, C
CGAGCCTGTT	−5.8	23	4	ZAP70	Zeta-chain (TCR)-associated protein kinase 70 kDa
GCGTCCTGCC	−13.0	13	1	LAT	Linker for activation of T cells
Apoptosis					
CAAGATAAAT	9.0	1	9	MAGED1	Melanoma antigen family D, 1
GTGGACCCCA	8.0	1	8	PUF60	Poly-U binding splicing factor 60 kDa
AGACTAACCT	−2.0	32	16	GZMH	Granzyme H (cathepsin G-like 2, protein h-CCPX)
GAGACTTGAG	−2.6	23	9	ITGB2	Integrin, beta 2 (complement component 3 receptor 3 and 4 subunit)
GACTCTGGGA	−2.8	11	4	CLPTM1L	CLPTM1-like
GGGGGCGCCT	−3.0	9	3	SLC25A6	Solute carrier family 25 (mitochondrial carrier; adenine nucleotide translocator), member 6
TGTGTGGGGC	−3.0	9	3	RHOT2	Ras homolog gene family, member T2
GTGACAACAC	−8.0	8	1	VDAC1	Voltage-dependent anion channel 1
TGAAGCAGTA	−8.0	8	1	PDCD4	Programmed cell death 4 (neoplastic transformation inhibitor)
TGCCCCTGAA	−8.0	8	1	XAF1	XIAP-associated factor 1
Cell adhesion					
GAAGAGTTCC	5.7	3	17	LEF1	Lymphoid enhancer-binding factor 1
ATAGGTCAGA	4.0	3	12	CLSTN1	Calsyntenin 1
TGGAACTGTG	−2.0	16	8	SIGLEC8	Sialic acid binding Ig-like lectin 8
GAGACTTGAG	−2.6	23	9	ITGB2	Integrin, beta 2 (complement component 3 receptor 3 and 4 subunit)
TTGCCCAGCA	−2.7	16	6	CERCAM	Cerebral endothelial cell adhesion molecule
CCTCTAGAGG	−3.5	14	4	CCL5	Chemokine (C–C motif) ligand 5
CAAAAAAAAA	−13.0	13	1	ADA	Adenosine deaminase
Inflammatory response					
TGGGAGCTCA	8.0	1	8	NCR3	Natural cytotoxicity triggering receptor 3
TACCTGCAGA	−2.2	54	25	S100A8	S100 calcium binding protein A8
GAGACTTGAG	−2.6	23	9	ITGB2	Integrin, beta 2 (complement component 3 receptor 3 and 4 subunit)
CCTCTAGAGG	−3.5	14	4	CCL5	Chemokine (C–C motif) ligand 5
GCTGAACGCG	−3.0	9	3	CEBPB	CCAAT/enhancer binding protein (C/EBP), beta
Cytokine activity					
TAGAAAAATA	12.0	1	12	GPI	Glucose-6-phosphate isomerase
TTTATCTGCT	8.0	1	8	HMGB1	High-mobility group box 1
CCACTACACT	−3.5	14	4	TNFSF10	Tumor necrosis factor (ligand) superfamily, member 10
GAAATTTAAA	−3.0	9	3	HMGB1	High-mobility group box 1
TCTGCTAAAG	−13.0	13	1	HMGB1	High-mobility group box 1

HAC, HTLV-1-asymptomatic carriers; HAM/TSP, HTLV-1-associated myelopathy/tropical spastic paraparesis; FC, fold change. The tag sequence represents the 10-bp SAGE tag. Normalized frequencies were obtained using SAGE software by calculating the total number of 300,000.

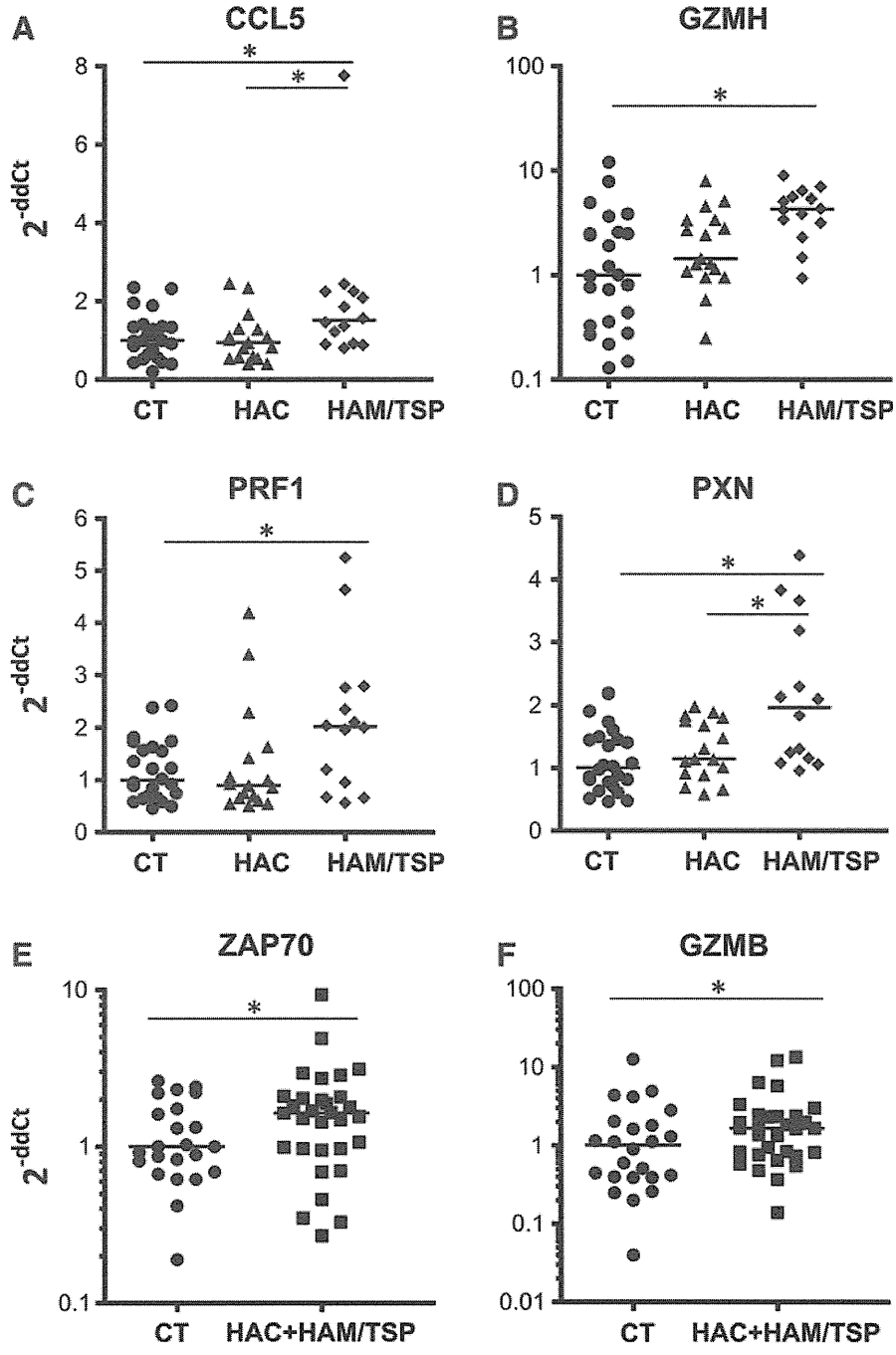

FIG. 2. Gene expression in CT, HAC, and HAM/TSP CD8$^+$ T cells using qRT-PCR. **(A)** CCL5, **(B)** GZMH, **(C)** PRF1, **(D)** PXN, **(E)** ZAP70, and **(F)** GZMB. The relative level of gene expression was obtained from the CT ($n=24$), HAC ($n=17$), and HAM/TSP ($n=14$) groups. Bars indicate the median of each group. The median of the CT group was used as a calibrator. Asterisks indicate p values <0.05 (*) compared with ANOVA. The Mann–Whitney test was used for comparison between the two groups. CT, control group; HAC, HTLV-1-asymptomatic carriers; and HAM/TSP, HTLV-1-associated myelopathy/tropical spastic paraparesis.

We also tested expression levels of GZMB and although no difference was observed among the CT, HAC, and HAM/TSP groups, we found a significant increase in whole infected patients (HAC+HAM/TSP) compared to the CT group (Fig. 2F).

PRF1 and GZMB protein levels were differentially expressed among HAC and HAM/TSP groups

To more directly confirm the results of gene expression data, we quantified proteins level of PRF1 and GZMB by quantitative flow cytometry. When we performed intracellular staining of PRF1, we detected significantly higher MFI in the HAM/TSP group compared to the HAC group (Fig. 3A). Moreover, the GZMB intracellular expression also revealed a significant increase of MFI in HAM/TSP patients than the HAC group, as shown in Fig. 3B.

Distinct correlation between gene expression and PVL

We considered if there was an association between PVL and the gene expression data and we saw no correlation among PVL and PRF1, GZMB, ZAP70, or PXN ($p>0,05$). However, PVL correlated positively with GZMH ($r=0.3947$, $p=0.0345$) and CCL5 ($r=0.5257$, $p=0.0060$).

Discussion

CD8$^+$ T cells play an important role in HTLV-1 infection and their frequency and efficiency are related to PVL levels,

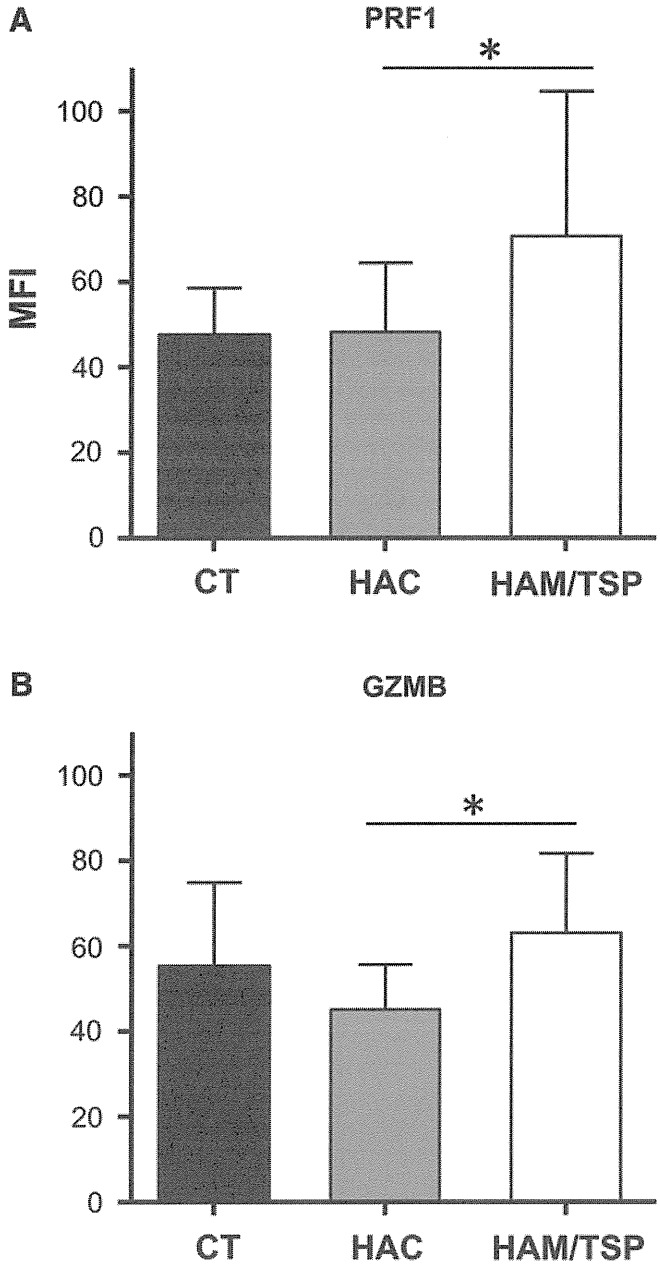

FIG. 3. Quantitative flow cytometry of PRF1 **(A)** and GZMB **(B)** in $CD8^+$ T cell populations from HTLV-1-infected patients and controls. MFI indicates the mean fluorescence intensity. Bars indicate the mean of each group with standard deviation. Asterisks indicate p values < 0.05 (*) compared with ANOVA. CT, control group; HAC, HTLV-1-asymptomatic carriers; and HAM/TSP, HTLV-1-associated myelopathy/tropical spastic paraparesis.

which in turn might be associated with HAM/TSP development. In our study, we found that a distinct gene expression profile of $CD8^+$ T cells between the HAC and HAM/TSP groups exists. Using SAGE methodology, we screened for some differentially expressed genes associated with a number of functional categories, including apoptosis, cytolysis, cytotoxicity, cellular development, growth and proliferation, immunological and neurological diseases, inflammatory response, and diseases and infection. Due to their potential biological role in HTLV-1 infection, we focus on cytotoxicity and cytokine-related genes and assessed the levels of expression of GZMB, GZMH, PRF1, ZAP70, PXN, and CCL5.

Our results showed that patients with HAM/TSP have high expression levels of genes related to cell-mediated lysis, namely GZMH and PRF1. Moreover, GZMH expression showed a significant positive correlation with PVL. In addition, we found that HTLV-infected patients (HAC + HAM/TSP) expressed higher levels of GZMB than the noninfected group (CT). In agreement with mRNA measurements, we detected higher protein expression levels of PRF1 and also of GZMB in HAM/TSP patients, compared to the HAC group.

$CD8^+$ T cells are responsible for combatting target cells bearing antigens recognized by the T cell receptor (TCR). When $CD8^+$ T cells encounter cells presenting HTLV antigens, they are supposed to release specialized granules containing cytolytic molecules, including perforin and granzymes, and to kill them. During HTLV-1 infection, overexpression of these cytolytic molecules, as we found here, might be explained as an effect of the vast antigen stimulus due to circulating infected cells, which is more prominent in HAM/TSP patients who have a high PVL. These findings suggest that $CD8^+$ T cells are activated during HTLV-1 infection, mainly in HAM/TSP patients, although they are not able to limit viral replication and control disease development.

In contrast to our results, Sabouri *et al.*[32] detected that HTLV-1-infected individuals express lower protein levels of PRF1 as compared to CT. The same study found that GZMB shows higher levels in the HAM/TSP group than in HAC, corroborating our data. Vine *et al.*[33] compared the gene expression of $CD8^+$ T cells from HTLV-1-infected individuals with low and high levels of PVL. They found that a number of genes related to cell-mediated lysis (including PRF1 and GZMB) were overexpressed in patients with low PVL, suggesting that there is an association between a strong cytotoxic $CD8^+$ T cell activity and an effective HTLV-1 suppression, which diverges from our findings.

At this point we cannot explain these apparently contrasting results. In fact, the investigation of PRF1 and granzyme expression is complex. $CD8^+$ T cell degranulation does not require new gene transcription and can occur within 30–60 min of stimulation[34] making mRNA and mainly protein measurement a challenge.

We also detected ZAP70 increased expression in HTLV-infected patients (HAC + HAM/TSP) compared to the noninfected group (CT), suggesting that $CD8^+$ T cells of HTLV-1-infected individuals are activated. ZAP70 is a protein tyrosine kinase associated with TCR, which is involved in signal transduction that leads to cell response upon TCR activation.[35] The high ZAP70 expression can also be an effect of the vast antigens circulating during infection, as we proposed for cytolytic altered genes.

Another cytokine investigated in our study was CCL5 (RANTES), with higher expression in the HAM/TSP group as compared to the HAC and CT groups. This cytokine is associated with immunomodulation and inflammatory processes. In agreement with our findings, several studies have demonstrated that elevation of CCL5 expression is observed in HTLV-1-infected cell lines, in peripheral blood cells, and in lymph nodes from HAM/TSP and ATLL patients.[36–38] High levels of this chemokine were also found in the cerebrospinal fluid from HTLV-1 patients.[38] It is likely that $CD8^+$ T cells from HTLV-1-infected individuals are somehow chronically activated,

probably in response to HTLV-1 antigens. Additionally, mediating leukocyte recruitment and T cell stimulation, CCL5 might play a role in HAM/TSP physiopathology.

At last, we detected an increase of PXN in the HAM/TSP group compared to the CT and to HAC groups. Paxillin is a cytoskeletal adaptor protein that plays an important role in cell adhesion and motility in adherent cells. During HIV-1 infection, PXN was described as a positive regulator of viral infection. In other words, PXN is involved in host cytoskeleton organization that allows viral entry in the target cell during virological synapse.[39] Additionally, in human cytomegalovirus infection, PXN regulation plays a role in the process of viral entry into monocytes and consequently in viral dissemination.[40] It is not clear what role PXN plays in T cells, but there is evidence that PXN is involved in CD8+ T cell degranulation in immunological synapse. Once TCR is activated, there is a microtubule organizing center reorientation, movement, and fusion of the cytolytic granules with the plasma membrane, with PXN involvement.[34] In this way, although there is no report of PXN participation in HTLV infection, as we found a high expression level of ZAP70 and of the cytolytic genes PRF and granzymes, we propose that PXN is overexpressed in HAM/TSP patients due to the intense granules releasing in the immunological synapses. PXN could also be involved in HTVL spread, although CD8+ T cells are not the main infected cells during the infection.

To investigate whether the gene expression differences found between the HAC and HAM/TSP groups were caused by the differences in PVL, we assessed the correlation between PVL and the gene expression data. We could not answer this question since half of the genes showed a correlation with PVL whereas the rest of them did not. The analysis of data with similar PVL and different clinical status would be useful to address the gene expression differences between the HAC and HAM/TSP conditions. However, in our cohort, we could not identify a group of HAC and HAM/TSP patients with similar PVL.

In this study, we analyzed the whole CD8+ T cell population, which comprises specific CD8+ T cells to a variety of antigens, including HTLV-1-specific CD8+ T cells, and also includes CD8+ T cells infected by HTLV-1. To identify genes involved in HTLV-1 infection, it would be preferable to study purified HTLV-1-specific CD8+ T cells; however, these cells were not isolated here because current quantification techniques of antigen-specific cells may modify gene expression. It is known that 10% of total circulating CD8+ T cells are HTLV-1-specific CD8+ T cells.[41] Thus, we believe that the gene expression profile generated here is most likely the result of virus-activated cells.

We also performed Tax protein quantification, which is a marker of proviral expression, to estimate the frequency of HTLV-1-infected CD8+ T cells capable of expressing Tax protein. We found that this frequency, despite being higher in HAM/TSP, was low in both groups, compared to the frequency of HTLV-1-infected CD4+ T cells (data not shown). Since HTLV-1-infected CD8+ T cells are not the main reservoir of HTLV-1 *in vivo*, we believe that the frequency of these cells did not undermine our results.

We found some discordant results among the different employed methodologies: SAGE, qRT-PCR, and flow cytometry. We understand that each methodology has its particularities and some inherent drawbacks, and we believe the main reason for our discordant findings is that we could not perform SAGE, qRT-PCR, and flow cytometry with the same number of samples.

Our findings showed that CD8+ T cells of HAM/TSP patients have an inflammatory and active profile. PXN and ZAP70 overexpression in HTLV-1-infected patients was described for the first time here and reinforces this concept. However, although active and abundant CD8+ T cells exist, they are not able to completely eliminate infected cells and prevent the development of HAM/TSP. Moreover, these active cells might contribute to the pathogenesis of the disease by migrating to the CNS, as we found deregulation of CCL5 expression in infected patients.

Our results provide a large-scale perspective of gene expression that should be further tested with biological functional assays to increase our understanding of the role these molecules play in the development of HTLV-1-related diseases.

Sequence Data

SAGE data have been deposited in the NCBI Gene Expression Omnibus (www.ncbi.nlm.nih.gov/geo/) (GEO ID: GSM641893 and GSM641894).

Acknowledgments

We thank Rochele Azevedo, Larissa Deadame de Figueiredo Nicolete, Rodrigo Haddad, Adriana Aparecida Marques, and Patricia Viana Bonini Palma for their assistance in laboratory techniques. We also thank Prof. Charles Bangham for training us in Tax expression analysis. The authors are also grateful to the patients. This work was supported by Fundação de Amparo a Pesquisa do Estado de São Paulo (FAPESP), Centro de Terapia Celular/Fundação Hemocentro de Ribeirão Preto (CTC/FUNDHERP), and Conselho Nacional de Desenvolvimento Científico e Tecnológico (CNPq), Brazil.

Author Disclosure Statement

No competing financial interests exist.

References

1. de The G and Bomford R: An HTLV-I vaccine: Why, how, for whom? AIDS Res Hum Retroviruses 1993;5:381–386.
2. Hinuma Y, Nagata K, Hanaoka M, *et al.*: Adult T-cell leukemia: Antigen in an ATL cell line and detection of antibodies to the antigen in human sera. Proc Natl Acad Sci USA 1981;78:6476–6480.
3. Yoshida M, Seiki M, Yamaguchi K, and Takatsuki K: Monoclonal integration of human T-cell leukemia provirus in all primary tumors of adult T-cell leukemia suggests causative role of human T-cell leukemia virus in the disease. Proc Natl Acad Sci USA 1984;81:2534–2537.
4. Gessain A, Barin F, Vernant JC, *et al.*: Antibodies to human T-lymphotropic virus type-I in patients with tropical spastic paraparesis. Lancet 1985;2:407–410.
5. Osame M, Usuku K, Izumo S, *et al.*: HTLV-I associated myelopathy, a new clinical entity. Lancet 1986;1:1031–1032.
6. LaGrenade L, Hanchard B, Fletcher V, Cranston B, and Blattner W: Infective dermatitis of Jamaican children: A marker for HTLV-I infection. Lancet 1990;336:1345–1347.
7. Mochizuki M, Ono A, Ikeda E, *et al.*: HTLV-I uveitis. J Acquir Immune Defic Syndr Hum Retrovirol 1996;13(Suppl 1):S50–56.
8. Morgan OS, Rodgers-Johnson P, Mora C, and Char G: HTLV-1 and polymyositis in Jamaica. Lancet 1989;2:1184–1187.
9. Kaplan JE, Osame M, Kubota H, *et al.*: The risk of development of HTLV-I-associated myelopathy/tropical spastic

paraparesis among persons infected with HTLV-I. J Acquir Immune Defic Syndr 1990;3:1096–1101.
10. Murphy EL, Hanchard B, Figueroa JP, *et al.*: Modelling the risk of adult T-cell leukemia/lymphoma in persons infected with human T-lymphotropic virus type I. Int J Cancer 1989; 43:250–253.
11. Bangham CR: HTLV-1 infections. J Clin Pathol 2000;53:581-586.
12. Bangham CR and Osame M: Cellular immune response to HTLV-1. Oncogene 2005;24:6035–6046.
13. Kashima S, Rodrigues ES, Azevedo R, *et al.*: DC-SIGN (CD209) gene promoter polymorphisms in a Brazilian population and their association with human T-cell lymphotropic virus type 1 infection. J Gen Virol 2009;90:927–934.
14. Gadelha SR, Junior Alcantara LC, Costa GC, *et al.*: Correlation between polymorphisms at interleukin-6 but not at interleukin-10 promoter and the risk of human T lymphotropic virus type I-associated myelopathy/tropical spastic paraparesis in Brazilian individuals. J Med Virol 2008;80:2141–2146.
15. Sabouri AH, Saito M, Lloyd AL, *et al.*: Polymorphism in the interleukin-10 promoter affects both provirus load and the risk of human T lymphotropic virus type I-associated myelopathy/tropical spastic paraparesis. J Infect Dis 2004;190:1279–1285.
16. Takenouchi N, Yamano Y, Usuku K, Osame M, and Izumo S: Usefulness of proviral load measurement for monitoring of disease activity in individual patients with human T-lymphotropic virus type I-associated myelopathy/tropical spastic paraparesis. J Neurovirol 2003;9:29–35.
17. Goon PK, Hanon E, Igakura T, *et al.*: High frequencies of Th1-type CD4(+) T cells specific to HTLV-1 Env and Tax proteins in patients with HTLV-1-associated myelopathy/tropical spastic paraparesis. Blood 2002;99:3335–3341.
18. Parker CE, Daenke S, Nightingale S, and Bangham CR: Activated, HTLV-1-specific cytotoxic T-lymphocytes are found in healthy seropositives as well as in patients with tropical spastic paraparesis. Virology 1992;188:628–636.
19. Jacobson S: Immunopathogenesis of human T cell lymphotropic virus type I-associated neurologic disease. J Infect Dis 2002;186(Suppl 2):S187–192.
20. Mosley AJ, Asquith B, and Bangham CR: Cell-mediated immune response to human T-lymphotropic virus type I. Viral Immunol 2005;18:293–305.
21. Pinto MT, Rodrigues ES, Malta TM, *et al.*: HTLV-1/2 seroprevalence and coinfection rate in Brazilian first-time blood donors: An 11-year follow-up. Rev Inst Med Trop Sao Paulo 2012;54:123–130.
22. De Castro-Costa CM, Araujo AQ, Barreto MM, *et al.*: Proposal for diagnostic criteria of tropical spastic paraparesis/HTLV-I-associated myelopathy (TSP/HAM). AIDS Res Hum Retroviruses 2006;22:931–935.
23. Miley WJ, Suryanarayana K, Manns A, *et al.*: Real-time polymerase chain reaction assay for cell-associated HTLV type I DNA viral load. AIDS Res Hum Retroviruses 2000;16:665–675.
24. Lee B, Tanaka Y, and Tozawa H: Monoclonal antibody defining tax protein of human T-cell leukemia virus type-I. Tohoku J Exp Med 1989;157:1–11.
25. Velculescu VE, Zhang L, Vogelstein B, and Kinzler KW: Serial analysis of gene expression. Science 1995;270:484–487.
26. Pinheiro DG, Galante PA, de Souza SJ, Zago MA, and Silva WA Jr: A score system for quality evaluation of RNA sequence tags: An improvement for gene expression profiling. BMC Bioinform 2009;10:170.
27. Audic S and Claverie JM: The significance of digital gene expression profiles. Genome Res 1997;7:986–995.
28. Benjamini Y and Hochberg Y: Controlling the false discovery rate—;a practical and powerful approach to multiple testing. J R Stat Soc Ser B-Methodol 1995;57:289–300.
29. Hashimoto S, Suzuki T, Dong HY, Yamazaki N, and Matsushima K: Serial analysis of gene expression in human monocytes and macrophages. Blood 1999;94:837–844.
30. Vandesompele J, De Preter K, Pattyn F, *et al.*: Accurate normalization of real-time quantitative RT-PCR data by geometric averaging of multiple internal control genes. Genome Biol 2002;3:RESEARCH0034.
31. Pfaffl MW: A new mathematical model for relative quantification in real-time RT-PCR. Nucleic Acids Res 2001;29:e45.
32. Sabouri AH, Usuku K, Hayashi D, *et al.*: Impaired function of human T-lymphotropic virus type 1 (HTLV-1)-specific CD8+ T cells in HTLV-1-associated neurologic disease. Blood 2008;112:2411–2420.
33. Vine AM, Heaps AG, Kaftantzi L, *et al.*: The role of CTLs in persistent viral infection: Cytolytic gene expression in CD8+ lymphocytes distinguishes between individuals with a high or low proviral load of human T cell lymphotropic virus type 1. J Immunol 2004;173:5121–5129.
34. Robertson LK, Mireau LR, and Ostergaard HL: A role for phosphatidylinositol 3-kinase in TCR-stimulated ERK activation leading to paxillin phosphorylation and CTL degranulation. J Immunol 2005;175:8138–8145.
35. Fischer A, Picard C, Chemin K, Dogniaux S, le Deist F, and Hivroz C: ZAP70: A master regulator of adaptive immunity. Semin Immunopathol 2012;32:107–116.
36. Montanheiro P, Vergara MP, Smid J, da Silva Duarte AJ, de Oliveira AC, and Casseb J: High production of RANTES and MIP-1alpha in the tropical spastic paraparesis/HTLV-1-associated myelopathy (TSP/HAM). J Neuroimmunol 2007; 188:138–142.
37. Mori N, Krensky AM, Ohshima K, *et al.*: Elevated expression of CCL5/RANTES in adult T-cell leukemia cells: Possible transactivation of the CCL5 gene by human T-cell leukemia virus type I tax. Int J Cancer 2004;111:548–557.
38. Tanaka M, Matsushita T, Tateishi T, *et al.*: Distinct CSF cytokine/chemokine profiles in atopic myelitis and other causes of myelitis. Neurology 2008;71:974–981.
39. Brown C, Morham SG, Walsh D, and Naghavi MH: Focal adhesion proteins talin-1 and vinculin negatively affect paxillin phosphorylation and limit retroviral infection. J Mol Biol 2012;410:761–777.
40. Nogalski MT, Chan G, Stevenson EV, Gray S, and Yurochko AD: Human cytomegalovirus-regulated paxillin in monocytes links cellular pathogenic motility to the process of viral entry. J Virol 2012;85:1360–1369.
41. Bieganowska K, Hollsberg P, Buckle GJ, *et al.*: Direct analysis of viral-specific CD8+ T cells with soluble HLA-A2/Tax11-19 tetramer complexes in patients with human T cell lymphotropic virus-associated myelopathy. J Immunol 1999;162: 1765–1771.

Address correspondence to:
Simone Kashima
Regional Blood Center of Ribeirão Preto
Tenente Catão Roxo Street, 2501
14051-140 Ribeirão Preto
São Paulo
Brazil

E-mail: skashima@hemocentro.fmrp.usp.br

Potential Contribution of a Novel Tax Epitope–Specific CD4$^+$ T Cells to Graft-versus-Tax Effect in Adult T Cell Leukemia Patients after Allogeneic Hematopoietic Stem Cell Transplantation

Yotaro Tamai,* Atsuhiko Hasegawa,* Ayako Takamori,* Amane Sasada,* Ryuji Tanosaki,† Ilseung Choi,‡ Atae Utsunomiya,§ Yasuhiro Maeda,¶ Yoshihisa Yamano,‖ Tetsuya Eto,# Ki-Ryang Koh,** Hirohisa Nakamae,** Youko Suehiro,‡ Koji Kato,†† Shigeki Takemoto,‡‡ Jun Okamura,§§ Naokuni Uike,‡ and Mari Kannagi*

Allogeneic hematopoietic stem cell transplantation (allo-HSCT) is an effective treatment for adult T cell leukemia/lymphoma (ATL) caused by human T cell leukemia virus type 1 (HTLV-1). We previously reported that Tax-specific CD8$^+$ cytotoxic T lymphocyte (CTL) contributed to graft-versus-ATL effects in ATL patients after allo-HSCT. However, the role of HTLV-1–specific CD4$^+$ T cells in the effects remains unclear. In this study, we showed that Tax-specific CD4$^+$ as well as CD8$^+$ T cell responses were induced in some ATL patients following allo-HSCT. To further analyze HTLV-1–specific CD4$^+$ T cell responses, we identified a novel HLA-DRB1*0101–restricted epitope, Tax155–167, recognized by HTLV-1–specific CD4$^+$ Th1-like cells, a major population of HTLV-1–specific CD4$^+$ T cell line, which was established from an ATL patient at 180 d after allo-HSCT from an unrelated seronegative donor by in vitro stimulation with HTLV-1–infected cells from the same patient. Costimulation of PBMCs with both the identified epitope (Tax155–167) and known CTL epitope peptides markedly enhanced the expansion of Tax-specific CD8$^+$ T cells in PBMCs compared with stimulation with CTL epitope peptide alone in all three HLA-DRB1*0101$^+$ patients post–allo-HSCT tested. In addition, direct detection using newly generated HLA-DRB1*0101/Tax155–167 tetramers revealed that Tax155–167-specific CD4$^+$ T cells were present in all HTLV-1–infected individuals tested, regardless of HSCT. These results suggest that Tax155–167 may be the dominant epitope recognized by HTLV-1–specific CD4$^+$ T cells in HLA-DRB1*0101$^+$–infected individuals and that Tax-specific CD4$^+$ T cells may augment the graft-versus-Tax effects via efficient induction of Tax-specific CD8$^+$ T cell responses. *The Journal of Immunology*, 2013, 190: 4382–4392.

Human T cell leukemia virus type 1 (HTLV-1) is the causative agent of a highly aggressive CD4$^+$ T cell malignancy, adult T cell leukemia/lymphoma (ATL) (1, 2). This virus has infected 10–20 million people worldwide, especially in southern Japan, the Caribbean basin, South America, Melanesia, and equatorial Africa (3). Approximately 5% of HTLV-1–seropositive individuals develop ATL, and another 2–3% develop a slow progressive neurologic disorder known as HTLV-1–associated myelopathy/tropical spastic paraparesis (HAM/TSP) or various chronic inflammatory diseases (4). The majority of HTLV-1–infected individuals remain asymptomatic throughout their lives.

ATL is characterized by extremely poor prognosis, mainly because of intrinsic drug resistance to cytotoxic agents. It has been reported that allogeneic hematopoietic stem cell transplantation (allo-HSCT), but not autologous HSCT, improved the outcome of ATL (5, 6). In previous clinical studies carried out by the ATL allo-HSCT Study Group, the overall survival rate within 3 y after allo-HSCT with reduced intensity conditioning (RIC) was 36% (7). HTLV-1 proviral load became and remained undetectable in some ATL patients with complete remission after allo-HSCT, suggesting that it is an effective treatment for ATL (7–9). In these studies, we reported that donor-derived HTLV-1 Tax-specific CD8$^+$ CTLs were induced in some ATL patients who achieved complete remission after allo-HSCT (10). These CTLs were able to lyse recipient–derived HTLV-1–infected T cells in vitro, suggesting potential contributions to graft-versus-leukemia effects. CD8$^+$ T cells, especially CTLs, generally play an important role in controlling viral replication in various infections, such as those

*Department of Immunotherapeutics, Tokyo Medical and Dental University, Tokyo 113-8519, Japan; †Clinical Laboratories Division, National Cancer Center Hospital, Tokyo 104-0045, Japan; ‡Department of Hematology, National Kyushu Cancer Center, Fukuoka 811-1395, Japan; §Department of Hematology, Imamura Bun-in Hospital, Kagoshima 890-0064, Japan; ¶Division of Hematology, Department of Internal Medicine, Kinki University School of Medicine, Osaka 589-8511, Japan; ‖Department of Rare Diseases Research, Institute of Medical Science, St. Marianna University Graduate School of Medicine, Kawasaki 216-8512, Japan; #Department of Hematology, Hamanomachi Hospital, Fukuoka 810-8539, Japan; **Department of Hematology, Graduate School of Medicine, Osaka City University, Osaka 545-8585, Japan; ††Department of Medicine and Biosystemic Science, Kyushu University Graduate School of Medical Sciences, Fukuoka 812-8582, Japan; ‡‡Department of Hematology, National Hospital Organization Kumamoto Medical Center, Kumamoto 860-0008, Japan; and §§Institute for Clinical Research, National Kyushu Cancer Center, Fukuoka 811-1395, Japan

Received for publication October 26, 2012. Accepted for publication February 7, 2013.

This work was supported by grants from the Ministry of Health, Labor, and Welfare of Japan and the Ministry of Education, Culture, Sports, Science, and Technology of Japan.

Address correspondence and reprint requests to Dr. Atsuhiko Hasegawa, Department of Immunotherapeutics, Tokyo Medical and Dental University, Graduate School, 1-5-45 Yushima, Bunkyo-ku, Tokyo 113-8519, Japan. E-mail address: hase.impt@tmd.ac.jp

Abbreviations used in this article: AC, asymptomatic carrier; allo-HSCT, allogeneic stem cell transplantation; ATL, adult T cell leukemia/lymphoma; HAM/TSP, HTLV-1–associated myelopathy/tropical spastic paraparesis; HTLV-1, human T cell leukemia virus type 1; ILT, IL-2–dependent T cell line; LCL, lymphoblastoid B cell line; rhIL-2, recombinant human IL-2; RIC, reduced intensity conditioning; Treg, regulatory T.

www.jimmunol.org/cgi/doi/10.4049/jimmunol.1202971

involving HIV, hepatitis B virus, and hepatitis C virus. In HTLV-1 infection, HTLV-1–specific $CD8^+$ T cells predominantly recognize the Tax Ag and are believed to contribute to controlling infected cells (11, 12). A high frequency of functional Tax-specific $CD8^+$ T cells can be detected in HAM/TSP patients and some asymptomatic carriers (ACs), whereas most ATL patients and a small population of ACs show severely reduced Tax-specific $CD8^+$ T cell responses (13, 14). The mechanism underlying the suppression of HTLV-1–specific $CD8^+$ T cell responses in these patients has not yet been fully elucidated.

For induction and maintenance of virus-specific CTLs, virus-specific $CD4^+$ Th cell responses are required in many virus infections (15–19). However, there are only a few reports of HTLV-1–specific Th cell responses (20–23), presumably because of their susceptibility to HTLV-1 infection in vivo and in vitro (24). Preferential HTLV-1 infection in HTLV-1–specific $CD4^+$ T cells could be one of the reasons for immune suppression in ATL patients. In addition, it has been reported that a higher frequency of $CD4^+FOXP3^+$ regulatory T (Treg) cells is observed in infected individuals compared with uninfected healthy donors. The frequency of Tax^- Treg cells, which are a major population of Treg cells in infected individuals, is negatively correlated with HTLV-1–specific CTL responses (25). HTLV-1 basic leucine zipper factor might also be involved in immune suppression, because HTLV-1 basic leucine zipper was constitutively expressed in infected cells (26) and inhibited the activity of IFN-γ promoters by suppressing NFAT and AP-1 signaling pathways, resulting in the impaired secretion of Th1 cytokines from $CD4^+$ Th cells in a transgenic mouse model (27) These reports suggest that both the dysfunction of HTLV-1–specific $CD4^+$ Th cells and the increased number of uninfected Treg cells might be implicated in the immunosuppression observed in ATL patients. Conversely, in HAM/TSP patients, $CD4^+$ T cells are predominantly found in early active inflammatory spinal cord lesions (28, 29) with spontaneous production of proinflammatory, neurotoxic cytokines, such as IFN-γ and TNF-α (30), suggesting their contributions to the pathogenesis of HAM/TSP. However, the precise roles of HTLV-1–specific $CD4^+$ T cells in HTLV-1 infection remain unclear.

In some ATL patients who achieved complete remission after allo-HSCT, it has been suggested that donor-derived HTLV-1 Tax-specific CTLs may contribute to elimination of ATL cells (graft-versus-Tax effects) (10). We believe that $CD4^+$ T cells also play a critical role in the graft-versus-ATL effects because $CD4^+$ T cells are required for induction and maintenance of optimal CTL responses (15–19). It therefore is important to clarify the role of HTLV-1–specific $CD4^+$ T cells in the effects for understanding HTLV-1–specific T cell immunity in ATL patients after allo-HSCT and for developing new vaccine strategies to prevent recurrence of ATL.

Several studies have reported some HTLV-1–specific $CD4^+$ T cell epitopes restricted by different HLA haplotypes (20–23). The helper functions of these epitopes in HTLV-1–specific CTL responses in HTLV-1–infected individuals have not been well understood. However, Jacobson et al. (20) showed that $CD4^+$ T cells specific for Env gp46 196–209, an epitope restricted by HLA-DQ5 or -DRw16, exhibited a cytotoxic function by directly recognizing HTLV-1–infected cells. This observation raises the possibility that some HTLV-1–specific $CD4^+$ T cells may contribute to the graft-versus-ATL effects through their cytotoxic function in ATL patients after allo-HSCT.

In the current study, we demonstrated that both $CD4^+$ and $CD8^+$ Tax-specific T cell responses were induced in patients after allo-HSCT with RIC for ATL. To further analyze HTLV-1–specific $CD4^+$ T cell responses in ATL patients after allo-HSCT, we determined a novel HLA-DRB1*0101–resricted epitope, Tax155–167, recognized by HTLV-1–specific $CD4^+$ Th1-like cells, a major population of HTLV-1–specific $CD4^+$ T (T4) cell line, which was established from a patient in complete remission following allo-HSCT with RIC. Costimulation with oligopeptides corresponding to the Th1 epitope, Tax155–167, together with a known CTL epitope led to robust expansion of Tax-specific $CD8^+$ T cells in PBMCs from three HLA-DRB1*0101^+ patients after allo-HSCT tested. Furthermore, Tax155–167-specific $CD4^+$ T cells were found to be maintained in all HTLV-1–infected HLA-DRB1*0101^+ individuals tested, regardless of HSCT, by direct detection with newly generated HLA-DRB1*0101/Tax155–167 tetramers. Our results suggest that Tax155–167 may be a dominant epitope recognized by HTLV-1–specific $CD4^+$ T cells in HTLV-1–infected individuals carrying HLA-DRB1*0101 and that Tax-specific $CD4^+$ T cells may strengthen the graft-versus-ATL effects through efficient induction of Tax-specific CTL responses.

Materials and Methods

Subjects

A total of 18 ATL patients who underwent allo-HSCT with RIC regimen, and one HTLV-1–seronegative (#365) and two seropositive donors (one AC #310 and one HAM/TSP patient #294) carrying HLA-DRB1*0101 donated peripheral blood samples after providing written informed consent. Approximately one-half of these patients received allogeneic peripheral blood stem cell transplantation from HLA-A-, B-, and -DR–identical sibling donors. The other half received allogeneic bone marrow cells from HLA-A–, B–, and DR–identical seronegative unrelated donors (Table I). These patients were the participants of clinical studies organized by the ATL allo-HSCT Study Group, supported by the Ministry of Health, Welfare, and Labor of Japan. This study was also reviewed and approved by the Institutional Ethical Committee Review Board of the Tokyo Medical and Dental University.

Generation of cell lines derived from patients and donors

PBMCs were isolated using Ficoll-Paque PLUS (GE Healthcare, Buckinghamshire, U.K.) density gradient centrifugation and stored in liquid nitrogen in Bambanker stock solution (NIPPON Genetics, Tokyo, Japan) until required. These were used in part to obtain HTLV-1–infected IL-2–dependent T cell lines (ILT) and EBV-transformed lymphoblastoid B cell lines (LCL). ILT-#350 was spontaneously immortalized during long-term culture of PBMCs from patient #350 before allo-HSCT and maintained in RPMI 1640 medium (Life Technologies, Grand Island, NY) containing 20% FCS (Sigma Aldrich, St. Louis, MO) and 30 U/ml recombinant human IL-2 (rhIL-2; Shionogi, Osaka, Japan). LCL-#307, -#341, and -#350 were established by maintaining PBMCs from ATL patients #307, #341, and #350, respectively, after allo-HSCT. These PBMCs were maintained in RPMI 1640 medium containing 20% FCS, following infection with the EBV-containing culture supernatant of the B95-8 cell line, LCL-Kan, derived from a healthy individual was also used.

Synthetic peptides

A total of 18 overlapping peptides, 12- to 25-mer in length, spanning the central region of Tax (residues 103–246) were purchased and used for epitope mapping (Scrum Tokyo, Japan) (Table II). HLA-A*2402–restricted CTL epitopes (Tax301–309, SFHSLHLLF) (10) were used for in vitro stimulation of Tax-specific CTLs (Hokudo, Sapporo, Japan).

GST–Tax fusion protein–based immunoassay

HTLV-1 Tax-specific T cell responses were evaluated using GST–fusion proteins of the N-terminal (residues 1–127), central (residues 113–237), and C-terminal (residues 224–353) regions of HTLV-1 Tax (GST–Tax-A, -B, and -C, respectively) as described previously (13, 31). PBMCs (1×10^6 cells/ml) were incubated with or without a mixture of GST–Tax-A, -B, and -C proteins (GST–TaxABC) in 200 μl RPMI 1640 medium supplemented with 10% FCS. After 4 d, the supernatant was collected, and the concentration of IFN-γ in the supernatant was determined using an OptiEIA Human IFN-γ ELISA Kit (BD Biosciences, San Jose, CA). The minimum detectable dose for this assay was determined to be 23.5 pg/ml IFN-γ. $CD8^+$ cells were depleted from PBMCs by negative selection using Dynabeads M-450 CD8 (Invitrogen, Carlsbad, CA), according to the